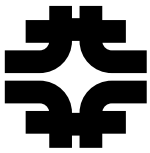

**Fermi National Accelerator Laboratory**

**FERMILAB-Conf-97/157-T**

# Hadron Colliders, the Top Quark and the Higgs Sector

Chris Quigg

*Fermi National Accelerator Laboratory*
*P.O. Box 500, Batavia, Illinois 60510*

July 1997

Presented at the *Advanced School on Electroweak Theory*, Mao, Menorca, Spain, June 17-21, 1996

Operated by Universities Research Association Inc. under Contract No. DE-AC02-76CH03000 with the United States Department of Energy

# HADRON COLLIDERS, THE TOP QUARK, AND THE HIGGS SECTOR

CHRIS QUIGG
*Fermi National Accelerator Laboratory*
*P. O. Box 500, Batavia, Illinois 60510 USA*
*and*
*Department of Physics, Princeton University*
*Princeton, New Jersey 08540 USA*

I survey the characteristics of hadron colliders as tools to investigate top-quark physics and to explore the 1-TeV scale of electroweak symmetry breaking.

## 1 Hadron Colliders for the 1-TeV Scale

Hadron colliders respond to our need to study a rich diversity of elementary processes at high energies. For orientation, let us suppose that we wish to study quark-quark collisions at a c.m. energy of 1 TeV. If we say that three quarks share one-half of a proton's momentum, *i.e.*, $\langle x \rangle = \frac{1}{6}$ for a quark, then we require proton-proton collisions at $\sqrt{s} \approx 6$ TeV.

To achieve this c.m. energy in a fixed-target machine would require a proton beam momentum $p \approx 2 \times 10^4$ TeV $= 2 \times 10^{16}$ eV, which approaches the momentum ($10^{19}$ to $10^{20}$ eV) of the highest-energy cosmic rays. The radius of a ring that magnetically confines a beam of momentum $p$ is

$$r = \frac{10}{3} \cdot \left(\frac{p}{1 \text{ TeV}}\right) / \left(\frac{B}{1 \text{ tesla}}\right) \text{ km.} \tag{1}$$

To confine a beam with $p = 2 \times 10^4$ TeV in conventional copper magnets with a field of $B = 2$ teslas would require a radius of

$$r \approx \tfrac{1}{3} \times 10^5 \text{ km.} \tag{2}$$

The distance from Earth to the Moon is about $4 \times 10^5$ km, so we see that the radius (2) is about $\frac{1}{12}$ the size of the Moon's orbit. A conventional fixed-target machine to explore the 1-TeV scale is a very large accelerator indeed! Superconducting magnets help—but not enough: a 10-tesla field reduces the size of the accelerator to mere Earth size ($R_\oplus = 6.4 \times 10^3$ km).

The solution—one of the great technological achievements of accelerator physics—is to collide one high-energy beam with another. Then to reach $\sqrt{s} =$

6 TeV, we need two 3-TeV proton synchrotrons, with radius

$$r_3 = \frac{10 \text{ teslas}}{B} \text{ km}. \tag{3}$$

For a 5-T magnetic field, well within current practice, the ring need only have a radius of $r_3 \approx 2$ km. Within some factor determined by the physics studies to be pursued in detail, this estimate defines the natural scale for a hadron collider to explore the 1-TeV scale. Because we have considered only quark-quark collisions, and have treated the proton very simply, this is a very rough estimate. Quark-antiquark, or glue-glue, or $WW$ collisions at 1 TeV will require a higher energy $pp$ machine. An estimate based on a circular ring is also an underestimate because accelerators need space for focusing magnets and for experiments—our reason for building the accelerators in the first place!

### *1.1 Hadron Colliders through the Ages*

The first hadron collider was the CERN Intersecting Storage Rings, which came into operation around 1970. The ISR was a $pp$ collider that eventually reached $\sqrt{s} = 63$ GeV. It was composed of two rings of conventional magnets.

About a decade later, the SPS Collider came into operation at CERN. Counter-rotating beams of protons and antiprotons were confined in a single conventional-magnet synchrotron (the CERN SPS) to provide collisions at $\sqrt{s} = 630$ GeV. The S$\bar{p}p$S Collider was home to the famous UA1 and UA2 detectors and a number of specialized experiments.

The Fermilab Tevatron, the first superconducting synchrotron, was commissioned in 1983. Like the S$\bar{p}p$S, the Tevatron is a proton-antiproton collider, with 900-GeV beams confined by 4-T magnets. The general-purpose CDF and DØ detectors and several specialized experiments have been installed in the Tevatron tunnel. In 1999, the energy of the Tevatron will be raised to 1 TeV per beam by cooling the magnets below 4 kelvins.

The Superconducting Super Collider (SSC) was to have been a $\sqrt{s} =$ 40 TeV proton-proton collider. With 6.6-T magnets, its circumference was 87 km. Alas, the United States abandoned construction in 1993.

The next machine on the horizon is the Large Hadron Collider (LHC) at CERN, a proton-proton collider under construction in the 27-km LEP tunnel. The LHC will be built of 9-T superconducting magnets operating at about 1.8 K, the temperature of superfluid helium. The LHC is our great hope for exploring the 1-TeV scale and unraveling the puzzle of electroweak symmetry breaking. Experiments may begin as early as 2005.

I should mention as well that the Relativistic Heavy Ion Collider (RHIC) at Brookhaven will have for part of each year (polarized) proton-proton collisions

at $\sqrt{s} = 400$ GeV. RHIC is a pair of superconducting rings with modest magnetic field.

### *1.2 Key Advances in Accelerator Technology*

Our ability to contemplate experiments at very high energies is owed to many important advances in accelerator technology. I would list six as being of defining importance:

- The idea of colliding beams.
- Alternating-gradient ("strong") focusing, invented by Christofilos, Courant, Livingston, and Snyder.
- Superconducting accelerator magnets. We owe to materials scientists the discovery of practical "type-II" superconductors, including the NbTi used in all superconducting machines to date, and the brittle $Nb_3Sn$, which may find use in special applications. The superconducting cable used in accelerator magnets has roots in pioneering work carried out at the Rutherford Laboratory, and essential early steps in the development of robust magnet structures were taken at Fermilab.
- The evolution of vacuum technology. Accelerator beams stored for approximately 20 hours must travel approximately $2 \times 10^{10}$ km, about 150 times the distance from Earth to Sun, without encountering a stray air molecule.
- The development of large-scale cryogenic technology, to maintain many kilometers of magnets at a few kelvins.
- We owe the S$\bar{p}p$S and Tevatron colliders to the development of intense antiproton sources, building on the work of Budker at Novosibirsk and van der Meer at CERN.

We would of course be nowhere without dreams and fantasies. I show in Figure 1 an artifact from my days in the SSC Central Design Group in Berkeley.

### *1.3 Competing Technologies*

There are no competing technologies, broadly speaking, if we wish to study collisions of quarks and gluons. There are, of course, many design choices to make, within the general framework of a hadron collider: $pp$ *vs.* $\bar{p}p$, low-field magnets *vs.* high-field magnets, *etc.*

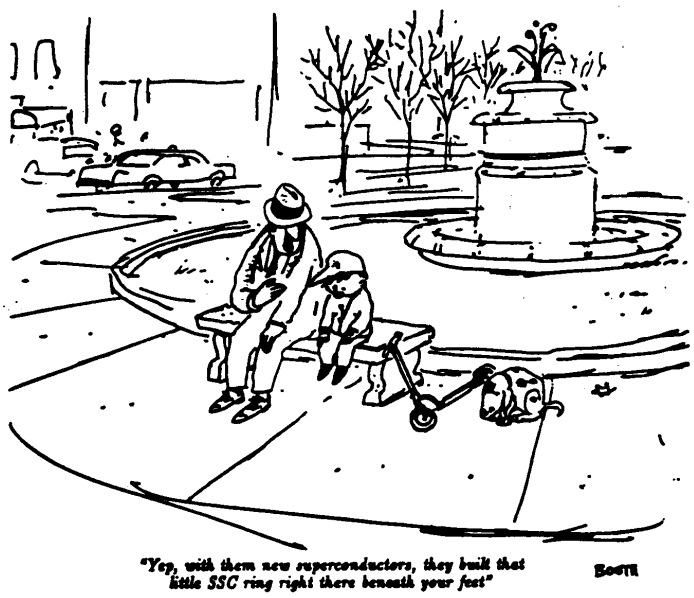


Figure 1: Illustration for the poster advertising a talk on high-$T_c$ superconductors at the SSC Central Design Group.

For the study of lepton-lepton scattering, LEP is the shining example of a (reasonably) high-energy $e^+e^-$ collider. It is widely agreed that the rise of synchrotron radiation causes circular electron machines to become impractical for energies above a few hundred GeV. Linear colliders, discussed at this school by Ramón Miquel,[1] are therefore under development for $\sqrt{s}$ from a few hundred GeV to about 1.5 TeV. The central question for linear colliders is, what performance at what cost? I think it possible that linear-collider technology may only be interesting for about one decade in energy; the growth path beyond 1 to 2 TeV is not clear. But it is a very interesting decade, the one on which we expect to learn the secrets of electroweak symmetry breaking, which is why there is such intense interest in the technology.

Over the past few years, the possibility of a muon collider has received increased attention.[2] The muon's brief lifetime (2.2 $\mu$s at rest) means that one imperative is to move fast! If a muon collider is practical, it may be attractive for lepton-lepton collisions at far higher energies than we contemplate for electron-positron machines, since the greater mass of the muon ($m_\mu \gg m_e$) means that synchrotron radiation is a minor concern. The muon collider is the

least developed technology of the hadron, electron, and muon alternatives, but it is not obviously impossible.

## 2 What Landmarks Do We Expect?

We have already remarked in the Introduction on the importance of the 1-TeV scale.[3] In this section, we wish to review for the first time some of the arguments that lead to an identification of the 1-TeV scale as a key landmark. As we shall see again and again in different ways, our understanding of the spontaneous breaking of the electroweak gauge symmetry is incomplete. A more complete understanding can be obtained only with the aid of a thorough knowledge of what takes place on the 1-TeV scale.

Let us review the essential elements of the $SU(2)_L \otimes U(1)_Y$ electroweak theory.[4] To save writing, we shall speak of the model as it applies to a single generation of leptons. In this form, the model is neither complete nor consistent: anomaly cancellation requires that a doublet of color-triplet quarks accompany each doublet of color-singlet leptons. However, the needed generalizations are simple enough to make that we need not write them out.

We begin by specifying the fermions: a left-handed weak isospin doublet

$$\mathsf{L} = \begin{pmatrix} \nu_e \\ e \end{pmatrix}_L \tag{4}$$

with weak hypercharge $Y_L = -1$, and a right-handed weak isospin singlet

$$\mathsf{R} \equiv e_R \tag{5}$$

with weak hypercharge $Y_R = -2$.

The electroweak gauge group, $SU(2)_L \otimes U(1)_Y$, implies two sets of gauge fields: a weak isovector $\vec{b}_\mu$, with coupling constant $g$, and a weak isoscalar $\mathcal{A}_\mu$, with coupling constant $g'$. Corresponding to these gauge fields are the field-strength tensors $\vec{F}_{\mu\nu}$ for the weak-isospin symmetry and $f_{\mu\nu}$ for the weak-hypercharge symmetry.

We may summarize the interactions by the Lagrangian

$$\mathcal{L} = \mathcal{L}_{\text{gauge}} + \mathcal{L}_{\text{leptons}} \ , \tag{6}$$

with

$$\mathcal{L}_{\text{gauge}} = -\frac{1}{4} F^{\ell}_{\mu\nu} F^{\ell\mu\nu} - \frac{1}{4} f_{\mu\nu} f^{\mu\nu}, \tag{7}$$

and

$$\begin{aligned}\mathcal{L}_{\text{leptons}} &= \overline{\mathsf{R}}\, i\gamma^\mu\left(\partial_\mu + i\frac{g'}{2}\mathcal{A}_\mu Y\right)\mathsf{R} \\ &+ \overline{\mathsf{L}}\, i\gamma^\mu\left(\partial_\mu + i\frac{g'}{2}\mathcal{A}_\mu Y + i\frac{g}{2}\vec{\tau}\cdot\vec{b}_\mu\right)\mathsf{L}.\end{aligned} \tag{8}$$

To hide the electroweak symmetry, we introduce a complex doublet of scalar fields

$$\phi \equiv \begin{pmatrix} \phi^+ \\ \phi^0 \end{pmatrix} \tag{9}$$

with weak hypercharge $Y_\phi = +1$. Add to the Lagrangian new terms for the interaction and propagation of the scalars,

$$\mathcal{L}_{\text{scalar}} = (\mathcal{D}^\mu\phi)^\dagger(\mathcal{D}_\mu\phi) - V(\phi^\dagger\phi), \tag{10}$$

where the gauge-covariant derivative is

$$\mathcal{D}_\mu = \partial_\mu + i\frac{g'}{2}\mathcal{A}_\mu Y + i\frac{g}{2}\vec{\tau}\cdot\vec{b}_\mu\ , \tag{11}$$

and the potential interaction has the form

$$V(\phi^\dagger\phi) = \mu^2(\phi^\dagger\phi) + |\lambda|\,(\phi^\dagger\phi)^2. \tag{12}$$

We are also free to add a Yukawa interaction between the scalar fields and the leptons:

$$\mathcal{L}_{\text{Yukawa}} = -G_e\left[\overline{\mathsf{R}}(\phi^\dagger\mathsf{L}) + (\overline{\mathsf{L}}\phi)\mathsf{R}\right]. \tag{13}$$

The electroweak symmetry is spontaneously broken if the parameter $\mu^2 < 0$. The minimum energy, or vacuum state, may then be chosen to correspond to the vacuum expectation value

$$\langle\phi\rangle_0 = \begin{pmatrix} 0 \\ v/\sqrt{2} \end{pmatrix}, \tag{14}$$

where

$$\begin{aligned} v = \sqrt{-\mu^2/\,|\lambda|} &= \left(G_F\sqrt{2}\right)^{-\frac{1}{2}} \\ &\approx 246\ \text{GeV}\end{aligned} \tag{15}$$

is fixed by the low-energy phenomenology of charged current interactions.

The spontaneous symmetry breaking has several important consequences:

- Electromagnetism is mediated by a massless photon, coupled to the electric charge;

- The mediator of the charged-current weak interaction acquires a mass characterized by $M_W^2 = \pi\alpha/G_F\sqrt{2}\sin^2\theta_W$, where $\theta_W$ is the weak mixing angle;

- The mediator of the neutral-current weak interaction acquires a mass characterized by $M_Z^2 = M_W^2/\cos^2\theta_W$;

- A massive neutral scalar particle, the Higgs boson, appears, but its mass is not predicted;

- Fermions (the electron in our abbreviated treatment) can acquire mass.

It is well known that the Standard Model does not give a precise prediction for the mass of the Higgs boson. We can, however, use arguments of self-consistency to place plausible lower and upper bounds on the mass of the Higgs particle in the minimal model. A lower bound is obtained by computing[5] the first quantum corrections to the classical potential (12). Requiring that $\langle\phi\rangle_0 \neq 0$ be an absolute minimum of the one-loop potential yields the condition

$$\begin{aligned} M_H^2 &> 3G_F\sqrt{2}(2M_W^4 + M_Z^4)/16\pi^2 \\ &\gtrsim 7 \ \text{GeV}/c^2 \, . \end{aligned} \tag{16}$$

Unitarity arguments[6] lead to a conditional upper bound on the Higgs boson mass. It is straightforward to compute the amplitudes $\mathcal{M}$ for gauge boson scattering at high energies, and to make a partial-wave decomposition, according to

$$\mathcal{M}(s,t) = 16\pi \sum_J (2J+1) a_J(s) P_J(\cos\theta) \, . \tag{17}$$

Most channels "decouple," in the sense that partial-wave amplitudes are small at all energies (except very near the particle poles, or at exponentially large energies), for any value of the Higgs boson mass $M_H$. Four channels are interesting:

$$W_L^+W_L^- \quad Z_L^0Z_L^0/\sqrt{2} \quad HH/\sqrt{2} \quad HZ_L^0 \, , \tag{18}$$

where the subscript $L$ denotes the longitudinal polarization states, and the factors of $\sqrt{2}$ account for identical particle statistics. For these, the $s$-wave

amplitudes are all asymptotically constant (*i.e.*, well-behaved) and proportional to $G_F M_H^2$. In the high-energy limit,

$$\lim_{s \gg M_H^2} (a_0) \to \frac{-G_F M_H^2}{4\pi\sqrt{2}} \cdot \begin{bmatrix} 1 & 1/\sqrt{8} & 1/\sqrt{8} & 0 \\ 1/\sqrt{8} & 3/4 & 1/4 & 0 \\ 1/\sqrt{8} & 1/4 & 3/4 & 0 \\ 0 & 0 & 0 & 1/2 \end{bmatrix} . \tag{19}$$

Requiring that the largest eigenvalue respect the partial-wave unitarity condition $|a_0| \leq 1$ yields

$$M_H \leq \left( \frac{8\pi\sqrt{2}}{3G_F} \right)^{1/2} = 1 \text{ TeV}/c^2 \tag{20}$$

as a condition for perturbative unitarity.

If the bound is respected, weak interactions remain weak at all energies, and perturbation theory is everywhere reliable. If the bound is violated, perturbation theory breaks down, and weak interactions among $W^{\pm}$, $Z$, and $H$ become strong on the 1-TeV scale. This means that the features of strong interactions at GeV energies will come to characterize electroweak gauge boson interactions at TeV energies. We interpret this to mean that new phenomena are to be found in the electroweak interactions at energies not much larger than 1 TeV.

It is worthwhile to note in passing that the threshold behavior of the partial-wave amplitudes for gauge-boson scattering follows generally from chiral symmetry.[7] The partial-wave amplitudes $a_{IJ}$ of definite isospin $I$ and angular momentum $J$ are given by

$$\begin{aligned} a_{00} &\approx \quad G_F s/8\pi\sqrt{2} \quad \text{attractive,} \\ a_{11} &\approx \quad G_F s/48\pi\sqrt{2} \quad \text{attractive,} \\ a_{20} &\approx -G_F s/16\pi\sqrt{2} \quad \text{repulsive.} \end{aligned} \tag{21}$$

**Problem:** Because the most serious high-energy divergences of a spontaneously broken gauge theory are associated with the longitudinal degrees of freedom of the gauge bosons, which arise from auxiliary scalars, it is instructive to study the Higgs sector in isolation. Consider, therefore, the Lagrangian for the Higgs sector of the $SU(3)_c \otimes SU(2)_L \otimes U(1)_Y$ electroweak theory before the gauge couplings are turned on,

$$\mathcal{L}_{\text{scalar}} = (\partial^\mu \phi)^\dagger (\partial_\mu \phi) - \mu^2 (\phi^\dagger \phi) - |\lambda| \, (\phi^\dagger \phi)^2 .$$

(a) Choosing $\mu^2 < 0$, investigate the effect of spontaneous symmetry breaking. Show that the theory describes three massless scalars $(w^+, w^-, z^0)$ and one massive neutral scalar $(h)$, which interact according to

$$\begin{aligned}\mathcal{L}_{\rm int} &= -|\lambda|\, vh(2w^+w^- + z^2 + h^2) \\ &\quad -(|\lambda|/4)(2w^+w^- + z^2 + h^2)^2,\end{aligned}$$

where $v^2 = -\mu^2/|\lambda|$. In the language of the full electroweak theory, $1/v^2 = G_F\sqrt{2}$ and $\lambda = G_F M_H^2/\sqrt{2}$.
(b) Deduce the Feynman rules for interactions and compute the lowest-order (tree diagram) amplitude for the reaction $hz \to hz$.
(c) Compute the $J = 0$ partial-wave amplitude in the high-energy limit and show that it respects partial-wave unitarity only if $M_H^2 < 8\pi\sqrt{2}/G_F$.
[Reference: B. W. Lee, C. Quigg, and H. B. Thacker, *Phys. Rev.* $D$**16**, 1519 (1977).]

## 3 What is a proton?

For the construction of large accelerators, we are limited to beams of charged, stable particles, which means to electrons and protons. With current methods, it is feasible to produce intense proton beams of tens of TeV, but electron beams of only about a tenth of a TeV. So far as we know, the electron is an elementary point particle ($r_e \lesssim 10^{-16}$ cm), but the proton is a composite system. Our ability to exploit the energy advantage of proton beams therefore depends on our knowledge of what a proton is, and how it behaves in high energy collisions. The purpose of this section is to summarize the state of our knowledge.

The static properties of a proton are well characterized by a description of a proton as a three-quark ($uud$) bound state, with a radius $r_p \approx 1$ fm. This picture accounts for the essential features of magnetic moments, axial charges, electromagnetic form factors, and such.[8]

What we might call the quasistatic properties of a proton are attributes measured in hard-scattering processes, but determined by low-energy (nonperturbative) dynamics. I have in mind the flavor-asymmetry of the light-quark sea, $u_s(x) \neq d_s(x)$, which can be understood from the chiral dynamics of constituent quarks and Goldstone bosons;[9] and the spin structure of the proton.

In collision, especially for the purpose of hard scattering, a proton is a broad-band, unselected beam of quarks, antiquarks, and gluons, and possibly other constituents as well. The composition of this mixed beam depends on

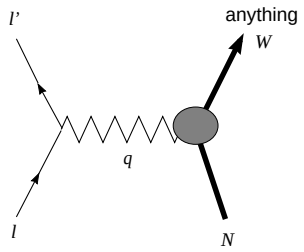


Figure 2: Kinematics of deeply inelastic scattering.

how you inspect it: the more virtual the probe, the more sensitive it will be to short time-scale fluctuations.

It is fruitful to analyze the proton in the framework of the *parton model* with QCD refinements. The fundamental quantity in this picture is $f_i^{(a)}(x_a, Q^2)$, the number density of partons of species $i$ with momentum fraction $x_a$ of hadron $a$ seen by a probe with resolving power characterized by $Q^2$.

Up to now, the best information on parton distributions (or hadron structure functions) comes from measurements of deeply inelastic lepton scattering, the reactions

$$eN \rightarrow e + \text{ anything}, \tag{22}$$

$$\mu N \rightarrow \mu + \text{ anything}, \tag{23}$$

$$\nu_\mu N \rightarrow \mu + \text{ anything}, \tag{24}$$

and

$$\nu_\mu N \rightarrow \nu_\mu + \text{ anything}. \tag{25}$$

For the scattering of charged leptons at present energies, the probe is a virtual photon (with usually negligible corrections for the exchange of a virtual $Z^0$). In the charged-current reaction (24), the nucleon is probed by $W^\pm$; in the neutral-current reaction (25), the probe is the $Z^0$.

The kinematic notation for deeply inelastic scattering is indicated in Figure 2. From the four-momenta indicated there we may form the useful invariants

$$s = (\ell + P)^2, \tag{26}$$

$$Q^2 \equiv -q^2 = -(\ell - \ell')^2, \tag{27}$$

$$\nu = q \cdot P/M, \tag{28}$$

where $M$ is the target mass, and

$$W^2 = 2M\nu + M^2 - Q^2 \tag{29}$$

is the square of the invariant mass of the produced hadronic system " anything." It is convenient to work in terms of Bjorken's dimensionless variables

$$x = Q^2/2M\nu, \tag{30}$$

the momentum fraction of the struck parton, and

$$y = \nu/E_{\rm lab}, \tag{31}$$

the fractional energy loss of the leptons in the laboratory frame.

For electromagnetic scattering, we may write the differential cross section as

$$\frac{d\sigma}{dxdy} = \frac{4\pi\alpha^2 s}{Q^4}\left[F_2(x)(1-y) + F_1(x)xy^2\right]. \tag{32}$$

In the parton model, $2xF_1(x) = F_2(x)$, and the structure function $F_2$ of the proton may be written as

$$F_2^{ep}(x)/x = \tfrac{4}{9}\left(u(x) + \overline{u}(x)\right) + \tfrac{1}{9}\left(d(x) + \overline{d}(x)\right) + \tfrac{1}{9}\left(s(x) + \overline{s}(x)\right) + \ldots \tag{33}$$

The structure function of the neutron is obtained by an isospin rotation, which is to say, by the replacement $u \leftrightarrow d$. The parton distributions satisfy the momentum sum rule,

$$\sum_{i=\substack{\text{parton}\\\text{species}}} \int_0^1 dx x f_i(x) = 1. \tag{34}$$

An important early result was the recognition that charged partons do not carry all the momentum of the nucleon. We may see this by approximating

$$F_2^{ep}(x) + F_2^{en}(x) = \tfrac{5}{9}x\left(u(x) + \overline{u}(x) + d(x) + \overline{d}(x)\right). \tag{35}$$

A measurement of $F_2$ then leads to an estimate of the momentum carried by charged partons through the connection

$$\begin{aligned} \tfrac{9}{5}\textstyle\int_0^1 dx\left(F_2^{ep}(x) + F_2^{en}(x)\right) &= \displaystyle\sum_{i=\substack{\text{quarks+}\\\text{antiquarks}}} \int_0^1 dx x f_i(x) \\ &= 0.45 \text{ experimental.} \end{aligned} \tag{36}$$

Unless most of the momentum of the nucleon is carried by strange (and heavier) quarks, this implies that about half the momentum of a proton is carried by neutrals.

Charged-current scattering of neutrinos from nucleons has also been studied extensively. We define an "isoscalar nucleon" $N \equiv \frac{1}{2}(p+n)$. The differential cross sections for scattering of neutrinos and antineutrinos are then

$$\frac{d\sigma(\nu N \to \mu^- + X)}{dxdy} = \frac{G_F^2 ME}{\pi}\left[(u(x)+d(x)) + \left(\overline{u}(x)+\overline{d}(x)\right)(1-y)^2\right], \tag{37}$$

$$\frac{d\sigma(\overline{\nu} N \to \mu^+ + X)}{dxdy} = \frac{G_F^2 ME}{\pi}\left[(u(x)+d(x))(1-y)^2 + \left(\overline{u}(x)+\overline{d}(x)\right)\right]. \tag{38}$$

The difference $\sigma(\nu N) - \sigma(\overline{\nu} N)$ allows a determination of the excess of quarks over antiquarks, *i.e.*, the distribution of "valence" quarks that determine the nucleon quantum numbers:

$$\Delta(x) \equiv u(x) - \overline{u}(x) + d(x) - \overline{d}(x) \equiv u_{valence} + d_{valence}. \tag{39}$$

Viewed at very long wavelengths, the proton appears structureless, but as $Q^2$ increases and the resolution becomes finer, the proton is revealed as a composite object characterized, for example, by rapidly falling elastic form factors that decrease as $1/Q^4$. According to the parton model, which ignores interactions among the constituents of the proton, the picture for deeply inelastic scattering is then exceedingly simple. Once $Q^2$ has become large enough for the quark constituents to be resolved, no finer structure is seen. The quarks are structureless, have no size, and thus introduce no length scale. When $Q^2$ exceeds a few GeV$^2$, all fixed mass scales become irrelevant and the structure functions and parton distributions do not depend upon $Q^2$. That this is approximately so in Nature may be seen from the measurements of $F_2^p(x, Q^2)$ shown in Figure 3.

In an interacting field theory, however, a more complex picture of hadron structure emerges. As $Q^2$ increases beyond the magnitude required to resolve quarks, the quarks themselves are found to have an apparent structure, which arises from the interactions mediated by the gluon fields. The parton distributions *evolve* with $Q^2$ as a result of quantum fluctuations. The virtual dissociation of a quark into a quark and gluon degrades the valence quark distribution. The virtual dissociation of a gluon into a $q\overline{q}$ pair enhances the population of quarks and antiquarks.

It is therefore plausible to expect, in any interacting field theory, that as $Q^2$ increases the structure function will fall at large values of $x$ and rise at small values of $x$. In most field theories, there is a power-law dependence on $Q^2$, but in asymptotically free gauge theories such as QCD, the dependence on $Q^2$ is

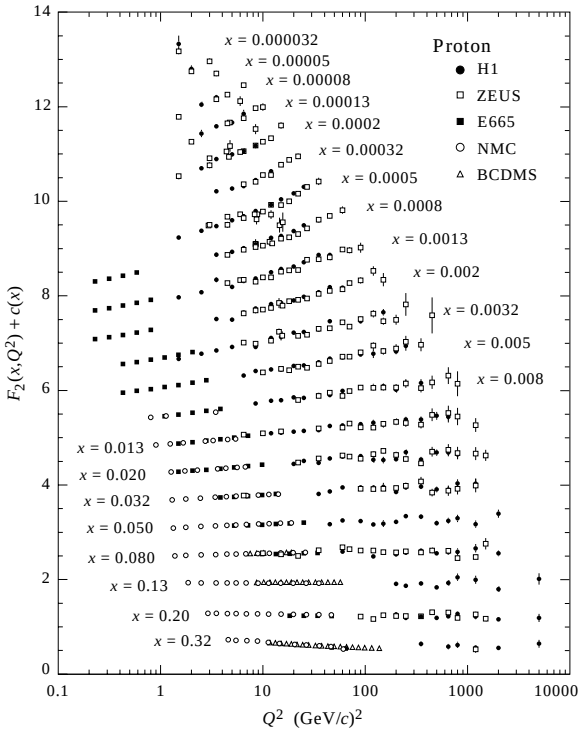


Figure 3: The proton structure function $F_2^p$ measured in electron (H1, ZEUS) and muon (BCDMS, E665, NMC) scattering [from the 1996 *Review of Particle Physics* [10]].

only logarithmic. The $Q^2$-evolution of the up-quark distribution $xu(x, Q^2)$ in the CTEQ4 parton distributions [11] is shown in Figure 4.

The flavor "nonsinglet" structure function

$$x\mathcal{F}_3^{\nu N} = x\left[u(x) - \overline{u}(x) + d(x) - \overline{d}(x)\right], \tag{40}$$

measures the valence quark distribution. It is of special interest because it receives no contribution from the dissociation of gluons into quark-antiquark pairs; it is simply degraded, with increasing $Q^2$, by gluon radiation from the valence quarks. It therefore offers, in principle, a means for studying the evolution of the quark distributions uncomplicated by the need to know anything about the gluon distribution.

Once parton distributions have been measured in detail at some value of $Q^2 = Q_0^2$, and the running coupling constant $\alpha_s(Q^2)$ of the strong interactions

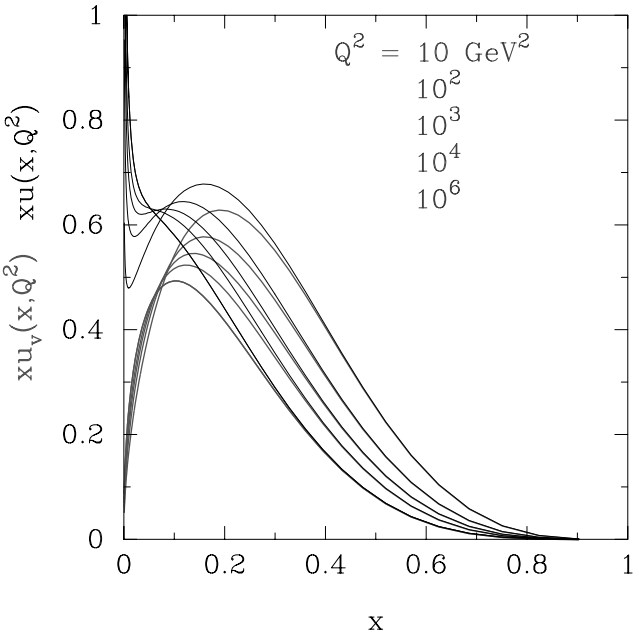


Figure 4: The up-quark distribution $xu(x, Q^2)$ in the proton for several values of $Q^2$, according to the CTEQ4 parton distribution functions.

has been determined, QCD permits us to compute the parton distributions at higher values of $Q^2$. A convenient formalism is provided by the Altarelli-Parisi equations,[12] integro-differential equations for the parton distributions.[13] It is worth recalling a few of the essentials here.

It is conventional to parameterize the strong coupling constant as

$$1/\alpha_s(Q^2) = \frac{33 - 2n_f}{12\pi} \ln(Q^2/\Lambda^2), \tag{41}$$

where $n_f$ is the number of "active" quark flavors, and to determine $\Lambda$ from the evolution of structure functions. For example, if we define the second moment

$$\Delta_2(Q^2) = \int_0^1 dx x \left[u_v(x) + d_v(x)\right] \tag{42}$$

of the valence quark distribution, then the Altarelli-Parisi equations give

$$\frac{\Delta_2(Q^2)}{\Delta_2(Q_0^2)} = \left[\frac{\alpha_s(Q_0^2)}{\alpha_s(Q^2)}\right]^{6A_2/(33-2n_f)}, \tag{43}$$

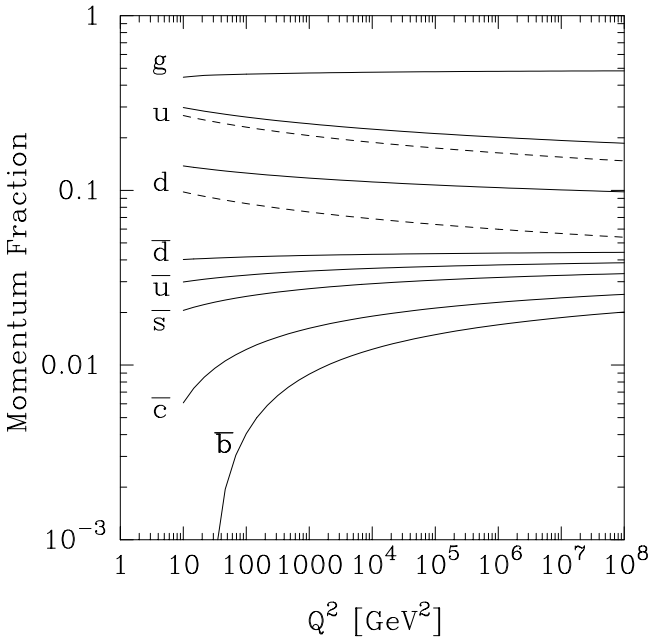


Figure 5: $Q^2$-evolution of the momentum fractions carried by various parton species.

where $A_2 \simeq 1.78$. Knowing $\int_0^1 dx x\mathcal{F}_3(x,Q^2)$ at different values of $Q^2$ thus allows, in principle, a direct determination of the QCD scale parameter $\Lambda$. In practice, the limited statistics of neutrino experiments, the small available range in $\ln(Q^2)$, and other factors limit the precision of such determinations.

If the evolution of $F_2^{\mu N}$ or $\mathcal{F}_2^{\nu N}$, either of which is measured with higher statistics than $x\mathcal{F}_3^{\nu N}$, is to be used for a determination of $\Lambda$, we are faced with the problem that the gluon distribution is not measured directly in lepton scattering. Its character must be inferred from the behavior of the antiquark distribution, and so is coupled with the value of $\Lambda$.

As a final response to our question, "What is a proton?" let us look at the flavor content of the proton, as measured by the momentum fraction

$$\int_0^1 dx x f_i(x,Q^2) \tag{44}$$

carried by each parton species. This is shown in Figure 5 for the CTEQ4 parton distributions.[11] As $Q^2$ increases, momentum is shared more and more equally among the quark and antiquark flavors, reflecting the trend toward the

asymptotic values

$$\begin{aligned}
\int_0^1 dx x G(x, Q^2 \to \infty) &= \tfrac{8}{17}, \\
\int_0^1 dx x q_s(x, Q^2 \to \infty) &= \tfrac{3}{68} \text{ (each flavor)}, \\
\int_0^1 dx x q_v(x, Q^2 \to \infty) &= 0,
\end{aligned} \tag{45}$$

expected in QCD with six quark flavors and no light colored superpartners. It is easy to verify that the momentum sum rule (34) is satisfied:

$$\tfrac{8}{17} + 6 \text{ flavors} \cdot 2 \text{ (quarks+antiquarks)} \cdot \tfrac{3}{68} = 1. \tag{46}$$

## 4 The Top Quark Must Exist

Ever since the existence of the $b$-quark was inferred from the discovery of the $\Upsilon$ family of resonances in 1977,[14] we have been on the lookout for its weak-isospin partner, called top. The long search, which occupied experimenters at laboratories around the world, came to a successful conclusion in 1995 with the announcement that the top quark had been observed in the CDF [15] and DØ [16] experiments at Fermilab.[17]

Although top has now been established and is under close experimental scrutiny, it is worth reviewing the arguments that convinced us that top had to exist. Even before we had direct experimental evidence for $b$ and $\tau$, M. Kobayashi and T. Maskawa [18] raised the possibility that $CP$ violation arises from complex elements of the quark mass matrix, if there are at least three fermion generations. Once the charge of the $b$-quark was established to be $e_b = -\frac{1}{3}$, it was natural to expect that the missing partner should be the upper member of a doublet, with charge $+\frac{2}{3}$. Completing the weak-isospin doublet by finding the top quark is the most natural way to cancel the anomaly of the $(\nu_\tau, \tau)_L$ doublet and ensure an anomaly-free electroweak theory.

The absence of flavor-changing neutral currents in $b$ decays, which would lead to significant branching fractions for dilepton channels such as $b \to s\ell^+\ell^-$, added phenomenological support to the idea that $b$ is a member of a left-handed weak doublet.

More recently, the accumulation of results on the neutral-current interactions of the $b$-quark has made it possible to characterize the $Zb\bar{b}$ vertex and measure the weak isospin of the $b$-quark. Consider a generalization of the $SU(2)_L \otimes U(1)_Y$ theory in which the $b$-quark may carry both left-handed and

right-handed weak isospin. The chiral neutral-current couplings can be written as

$$\begin{aligned} L_b &= I_{L3} - e_b \sin^2\theta_W \\ R_b &= I_{R3} - e_b \sin^2\theta_W \ , \end{aligned} \tag{47}$$

which differ from the standard-model chiral couplings by the presence of $I_{R3}$. Characteristics of the reaction $e^+e^- \to b\bar{b}$ permit us to determine the values of $I_{L3}$ and $I_{R3}$ directly from experiment. The partial width $\Gamma(Z^0 \to b\bar{b})$ measures the combination $L_b^2+R_b^2$. On the $Z^0$ resonance, the forward-backward asymmetry $A_{\rm FB}(Z^0 \to b\bar{b})$ measures the combination $(L_b^2-R_b^2)/(L_b^2+R_b^2)$. Far below the resonance, where the forward-backward asymmetry is dominated by $\gamma$-$Z$ interference, $A_{\rm FB}(e^+e^- \to b\bar{b})$ measures the combination $L_b - R_b$. The unique overlap of the allowed regions is for $I_{L3} = -\frac{1}{2}$, $I_{R3} = 0$, the standard-model solution.

## 5 Anticipating $m_t$

Little can be said on general theoretical grounds about the masses of new flavors, but interesting constraints arise from consistency requirements and from phenomenological relationships. Imposing the requirement that partial-wave unitarity be respected at the tree level in the reactions

$$Q\bar{Q} \to (W^+W^-, Z^0Z^0, HZ^0, HH) \tag{48}$$

leads to a condition on the heavy-quark mass $m_Q$, which determines the scale $(G_F m_Q^2\sqrt{2})^{1/2}$ of the $HQ\bar{Q}$ couplings.[19] For the $(t,b)_L$ doublet of heavy quarks, the restriction amounts to

$$|m_t - m_b| \lesssim 550 \text{ GeV}/c^2. \tag{49}$$

This general constraint can be sharpened appreciably by considering radiative corrections to electroweak observables.

Higher-order processes involving virtual top quarks are an important element in quantum corrections to the predictions the electroweak theory makes for many observables. A case in point is the total decay rate, or width, of the $Z^0$ boson, which has been measured to exquisite precision at the CERN and SLAC $Z$ factories. The comparison of experiment and theory shown in the inset to Figure 6 favors a top mass in the neighborhood of 180 GeV/$c^2$. The top mass favored by simultaneous fits to many electroweak observables is shown as a function of time in Figure 6.

Many other observables, particularly those related to neutral-meson mixing and $CP$ violation, are sensitive to the top-quark mass. One example, for

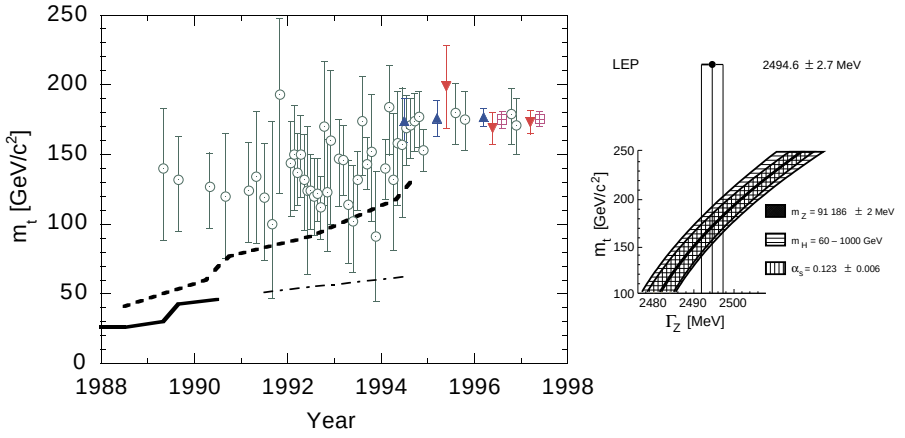


Figure 6: Indirect determinations of the top-quark mass from fits to electroweak observables (open circles) and 95% confidence-level lower bounds on the top-quark mass inferred from direct searches in $e^+e^-$ annihilations (solid line) and in $\bar{p}p$ collisions, assuming that standard decay modes dominate (broken line). An indirect lower bound, derived from the $W$-boson width inferred from $\bar{p}p \to (W \text{ or } Z) +$ anything, is shown as the dot-dashed line. Direct measurements of $m_t$ by the CDF (triangles) and DØ (inverted triangles) Collaborations are shown at the time of initial evidence, discovery claim, and today. The current world average from direct observations is shown as the crossed box. For sources of data, see Ref. [20]. *Inset:* Electroweak theory predictions for the width of the $Z^0$ boson as a function of the top-quark mass, compared with the width measured in LEP experiments (Ref. [21]).

which we may expect significant progress over the next five years, is the parameter $\epsilon'$ that measures direct $CP$ violation in the $K^0$-$\bar{K}^0$ system. Figure 7 shows the region favored by state-of-the-art calculations as a function of $m_t$.[22] We expect the theoretical uncertainty to shrink as lattice-QCD calculations mature. The values measured by E731 at Fermilab and by NA31 at CERN are plotted at arbitrary values of $m_t$.[23] The new generation of experiments may reduce the experimental uncertainty on $\epsilon'/\epsilon$ to $\pm 1 \times 10^{-4}$.

It is worth mentioning another hint that I have to confess seems more suggestive to me after the fact than it did before. In supersymmetric unified theories of the fundamental interactions, virtual top quarks can drive the spontaneous breakdown of electroweak symmetry—provided top is very massive.[24]

## 6 Production Rates

The calculation of the top-quark production cross section in perturbative QCD has been carried out to next-to-leading order (NLO) and beyond, using resum-

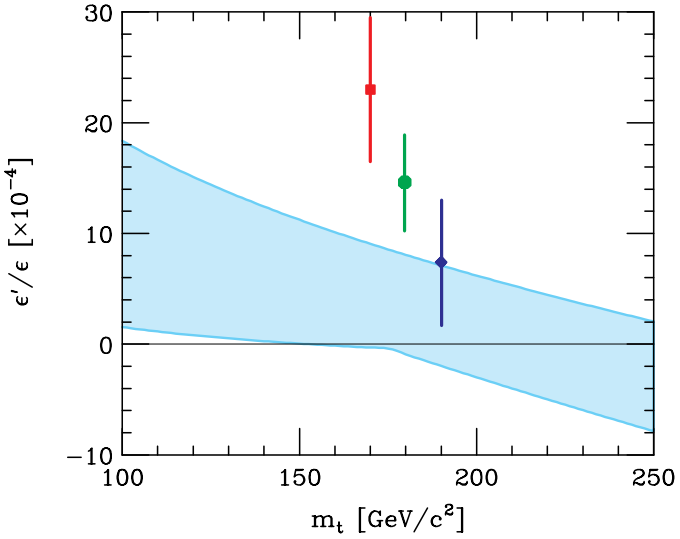


Figure 7: The quantity $\epsilon'/\epsilon$ in the standard model as a function of the top-quark mass. The band shows the region allowed by plausible variations in theoretical parameters. The values measured by NA31 (■) and E731(◆) are shown, together with the world average (●).

mation techniques.[25] Typical results are shown in Figure 8 for $p^{\pm}p$ collisions at c.m. energies between 1.8 and 14 TeV. At 1.8 TeV, for $m_t = 175$ GeV/$c^2$, the QCD cross section is $\sigma(\bar{p}p \to t\bar{t} + \text{ anything}) \approx 6$ pb, predominantly from the elementary process $\bar{q}q \to t\bar{t}$. At the level of $\pm 30\%$, there are differences among the competing calculations that need to be resolved. At 14 TeV, the energy planned for the Large Hadron Collider at CERN, the QCD cross section rises to $\sigma(pp \to t\bar{t} + \text{ anything}) \approx 800$ pb, predominantly from the mechanism $gg \to t\bar{t}$.

It is interesting to ask what would be gained by raising the top energy of the Tevatron collider by lowering the operating temperature of the superconducting magnets. Figure 9 shows how the top production cross section depends on $m_t$ at $\sqrt{s} = 1.8$ and 2.0 TeV, according to the resummed next-to-leading-order calculation of Laenen, Smith, and van Neerven.[27] For 160 GeV/$c^2 \le m_t \le$ 200 GeV/$c^2$, the cross section will increase by about 40% when the c.m. energy is raised to 2 TeV. The fraction of the cross section contributed by $gg$ collisions grows from about 15% to about 20% for a top-quark mass of 175 GeV/$c^2$. In addition to the dominant mechanisms for top production included in Figures 8 and 9, other conventional sources may take on

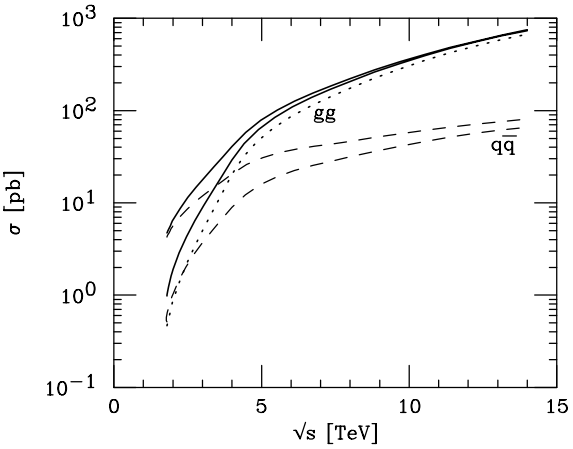


Figure 8: Energy dependence of the cross section for production of 175-GeV/$c^2$ top quarks in $pp$ (lower curves) and $\bar{p}p$ (upper curves) collisions. The contributions of $\bar{q}q$ (dashed curves) and $gg$ (dotted curve) collisions are shown separately. (After Parke, Ref. [26].)

importance as the integrated luminosity rises. I show in Figure 10 the contributions of the weak-interaction processes $W^+g \to t\bar{b}$ and (virtual) $q\bar{q} \to W^\star \to t\bar{b}$ to the cross section for producing $e^+ +$ jets, assuming that $t \to bW^+$ is top's only decay mode. The final state contains $e^+b\bar{b} + (2, 1, 0)$ non-$b$-quark jets for the QCD, $W$-gluon, and virtual-$W$ processes.

## 7 Top Width and Lifetime

In the standard model, the dominant decay of a heavy top quark is the semi-weak process $t \to bW^+$, for which the decay rate is [28]

$$\Gamma(t \to bW^+) = \frac{G_F M_W^2}{8\pi\sqrt{2}} \frac{1}{m_t^3} \left[ \frac{(m_t^2 - m_b^2)^2}{M_W^2} + m_t^2 + m_b^2 - 2M_W^2 \right] \times \sqrt{[m_t^2 - (M_W + m_b)^2][m_t^2 - (M_W - m_b)^2]}. \quad (50)$$

Here $m_t$, $m_b$, and $M_W$ are the masses of top, bottom, and the $W$-boson, and $V_{tb}$ measures the strength of the $t \to bW^+$ coupling. To the extent that the $b$-quark mass is negligible, the decay rate can be recast in the form

$$\Gamma(t \to bW^+) = \frac{G_F m_t^3}{8\pi\sqrt{2}} |V_{tb}|^2 \left(1 - \frac{M_W^2}{m_t^2}\right)^2 \left(1 + \frac{2M_W^2}{m_t^2}\right),$$

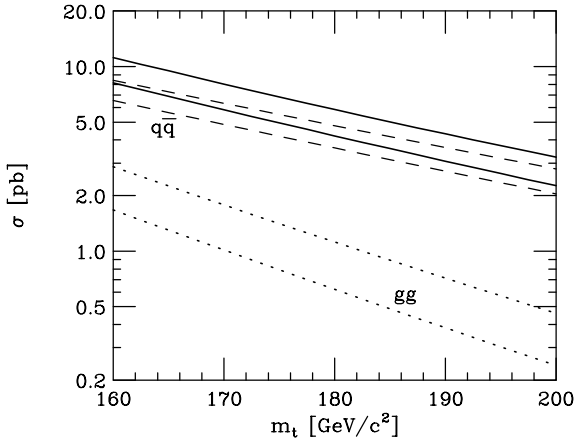


Figure 9: Dependence of the top production cross section, $\sigma(\bar{p}p \to t\bar{t} + \text{ anything})$, upon the top-quark mass in 1.8-TeV (lower curves) and 2.0-TeV (upper curves) $\bar{p}p$ collisions. The contributions of $q\bar{q}$ (dashed curves) and $gg$ (dotted curves) are shown separately.

which grows rapidly with increasing top mass.

If there are only three generations of quarks, so that the Cabibbo-Kobayashi-Maskawa matrix element $V_{tb}$ has a magnitude close to unity, then for a top-quark mass of 175 GeV/$c^2$, the partial width is

$$\Gamma(t \to bW^+) \approx 1.55 \text{ GeV}, \tag{51}$$

which corresponds to a top lifetime $\tau_t \approx 0.4 \times 10^{-24}$ s, or 0.4 yoctosecond (ys).[29] The confining effects of the strong interaction act on a time scale of a few yoctoseconds set by 1/the scale energy of quantum chromodynamics, $\Lambda_{\rm QCD}$. This means that a top quark decays long before it can be hadronized. There will be no discrete lines in toponium ($t\bar{t}$) spectroscopy, and indeed no dressed hadronic states containing top. Accordingly, the characteristics of top production and the hadronic environment near top in phase space should be calculable in perturbative QCD.[30]

The $t \to bW^+$ decay rate and (partial) lifetime are shown in Figure 11 for a range of top-quark masses.

It is noteworthy that top decay is an excellent source of longitudinally polarized $W$-bosons, which may be particularly sensitive to new physics. $W$-bosons with helicity $= -1$ are emitted with relative weight 1 and those with helicity $= 0$ are produced with relative weight $m_t^2/2M_W^2$. For $m_t = 180$ GeV/$c^2$, a fraction $f_0 = 71\%$ of the $W$-bosons emitted in top decay will be longitudinally

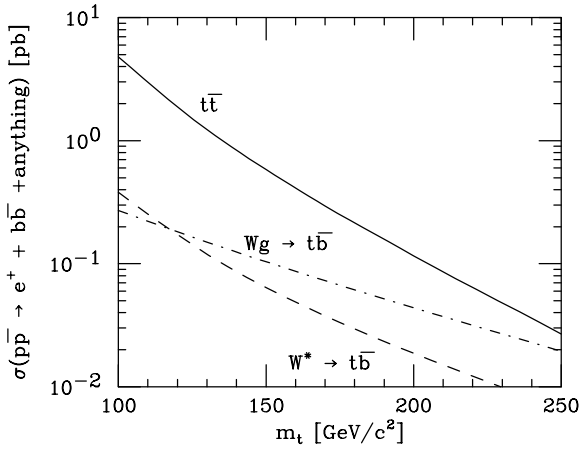


Figure 10: Variation of standard-model contributions to the cross section $\sigma(\bar{p}p \to e^+ b\bar{b} +$ jets) with the top-quark mass at $\sqrt{s} = 1.8$ TeV. Yields are shown for the $t\bar{t}$ (solid curve), $Wg \to t\bar{b}$ (dot-dashed curve), and $W^\star \to t\bar{b}$ (dashed curve) contributions. [After Parke, Ref. [26].]

polarized. The decay angular distribution of charged leptons in the $W$ rest frame is

$$\frac{d\Gamma(W^+ \to \ell^+ \nu_\ell)}{d(\cos\theta)} = \tfrac{3}{8}(1 - f_0)(1 - \cos\theta)^2 + \tfrac{3}{4} f_0 \sin^2\theta. \qquad (52)$$

## 8 Top Search and Discovery

Through the 1980s and early 1990s, direct searches continually raised the lower bound on the top mass, but produced no convincing sign of the top quark. The most stringent limits (Cf. Figure 6) came from the proton-antiproton colliders at CERN and Fermilab, but these relied on the assumption that top decays (almost) exclusively into a bottom quark and a real or virtual $W$ boson. Electron-positron colliders could look for $e^+e^- \to t\bar{t}$ without assumptions about the decay mechanism, but the lower energies of those machines led to rather weak bounds on $m_t$.

By 1994, an impressive body of circumstantial evidence pointed to the existence of a top quark with a mass of $175 \pm 25$ GeV/$c^2$. Finding top and measuring its mass directly emerged as a critical test of the understanding of weak and electromagnetic interactions built up over two decades.

The decisive experiments were carried out at Fermilab's Tevatron, in which a beam of 900-GeV protons collides with a beam of 900-GeV antiprotons.

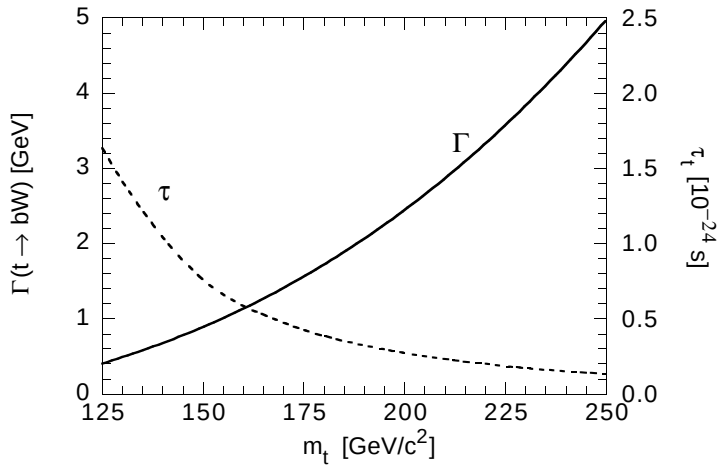


Figure 11: Partial width (solid curve, left-hand scale) for the decay $t \to bW^+$ as a function of $m_t$. The (partial) lifetime is shown as the dashed curve (right-hand scale). A full-strength $t \to b$ transition is assumed, and QCD corrections are omitted.

Creating top-antitop pairs in sufficient numbers to claim discovery demanded exceptional performance from the Tevatron, for only one interaction in ten billion results in a top-antitop pair. Observing traces of the disintegration of top into a $b$-quark and a $W$-boson required highly capable detectors and extraordinary attention to experimental detail. Both the $b$-quark and the $W$-boson are themselves unstable, with many multibody decay modes. The $b$-quark's mean lifetime is about 1.5 ps. It can be identified by a decay vertex displaced by a fraction of a millimeter from the production point, or by the low-momentum electron or muon from the semileptonic decays $b \to ce\nu$, $b \to c\mu\nu$, each with branching fraction about 10%. The $W$ boson decays after only 0.3 ys on average into $e\bar{\nu}_e$, $\mu\bar{\nu}_\mu$, $\tau\bar{\nu}_\tau$, or a quark and antiquark (observed as two jets of hadrons), with probabilities $\frac{1}{9}$, $\frac{1}{9}$, $\frac{1}{9}$, and $\frac{2}{3}$.

The first evidence for top was presented in April 1994 by the CDF Collaboration.[31] In a sample of 19.3 events per picobarn of cross section (19.3 pb$^{-1}$), CDF found 12 events consistent with either two $W$ bosons, or a $W$ boson and at least one $b$-quark. Although the sample lacked the statistical weight needed to claim discovery, the event characteristics were consistent with the $t\bar{t}$ interpretation, with a top mass of $174 \pm 10^{+13}_{-12}$ GeV/$c^2$. A few months later, the DØ Collaboration reported an excess of candidates (9 events with an expected background of $3.8 \pm 0.9$) in a 13.5-pb$^{-1}$ sample.[32]

The discovery was not far behind. By February 1995, both groups had quadrupled their data sets. The CDF Collaboration found 6 dilepton candidates with an anticipated background of $1.3 \pm 0.3$ events, plus 37 $b$-tagged events containing a $W$-boson and at least three jets.[15] The DØ Collaboration reported 17 top candidates with an expected background of $3.8 \pm 0.6$.[16] Taken together, the populations and characteristics of different event classes provided irresistible evidence for a top quark with a mass in the anticipated region: $176 \pm 8 \pm 10$ GeV/$c^2$ for CDF, and $199^{+19}_{-21} \pm 22$ GeV/$c^2$ for DØ. The top-antitop production rate was roughly in line with theoretical predictions.

Today, with the event samples approximately doubled again, the top mass is measured as $176.8 \pm 6.5$ GeV/$c^2$ by CDF and $173.3 \pm 8.4$ GeV/$c^2$ by DØ for a world average of $175.5 \pm 5.1$ GeV/$c^2$.[33] The production cross sections, $\sigma(\bar{p}p \to t\bar{t} + \text{anything}) = 5.53 \pm 1.67$ pb (DØ ) and $7.5^{1.9}_{1.6}$ pb (CDF) are close to what is expected.

The observation of top completes the last normal (light-neutrino) generation and provides a crucial parameter of the electroweak theory. The large mass of the top quark suggests that top might stand apart from the other quarks and leptons. Top provides a new window on novel physics through nonstandard production and decay. We now take up some of the implications of the discovery.

## 9 Top in Electroweak Radiative Corrections

The influence of the top quark on electroweak radiative corrections was the basis for the expectations for $m_t$ from precision measurements of electroweak observables. As the top-quark mass is known more precisely from direct measurements, it will be possible to compare predictions for which $m_t$ is an input with other observations. Over the next few years, we can anticipate incisive tests of the electroweak theory from the comparison of the $W$-boson mass with theoretical calculations.

The $W$-boson mass is given as

$$M_W^2 = M_Z^2(1 - \sin^2\theta_W)(1 + \Delta\rho), \tag{53}$$

where $M_Z$ is the mass of the $Z^0$ boson, $\sin^2\theta_W \approx 0.232$ is the weak mixing parameter, and $\Delta\rho$ represents quantum corrections. Some of the most important of these are shown at the top of Figure 12. The inequality of the $t$- and $b$-quark masses violates weak-isospin symmetry and results in

$$\Delta\rho = 3G_F m_t^2/8\pi^2\sqrt{2} + \ldots, \tag{54}$$

where the unwritten terms include a logarithmic dependence upon the mass of the Higgs boson, the hitherto undetected agent of electroweak symmetry breaking.

Predictions for $M_W$ as a function of the top-quark mass are shown in Figure 12 for several values of the Higgs-boson mass.[34] Current measurements are consistent with the electroweak theory, but do not yet provide any precise hints about the mass of the Higgs boson. The uncertainty on the world-average $M_W$ has now reached about 100 MeV/$c^2$. An uncertainty of $\delta M_W = 50$ MeV/$c^2$ seems a realistic possibility both at the Tevatron and at CERN's LEP200, where observations of the reaction $e^+e^- \to W^+W^-$ near threshold began in 1996. Improving $\delta m_t$ below 5 GeV/$c^2$ will then make for a demanding test of the electroweak theory that should yield interesting clues about the Higgs-boson mass. Over the next decade, it seems possible to reduce $\delta m_t$ to 2 GeV/$c^2$ at Fermilab and $\delta M_W$ to about 20 MeV/$c^2$ at the Tevatron and LEP200. That will set the stage for a crucial test of the electroweak theory when (and if) the Higgs boson is discovered.

## 10 Is It Standard Top?

The top-quark discovery channels all arise from the production of top-antitop pairs. We expect that all the significant channels will contain a $b\bar{b}$ pair, from the decay chain

$$\begin{array}{l} t\ \bar{t} \\ \left|\ \right\llcorner \to \bar{b}W^- \\ \left\llcorner \to bW^+\ , \right. \end{array} \tag{55}$$

leading to $b\bar{b}e^{\pm}\mu^{\mp}\nu\nu$, $b\bar{b}e^+e^-\nu\nu$, $b\bar{b}\mu^+\mu^-\nu\nu$, $b\bar{b}\ell\nu$ jet jet.

We expect that decays other than the observed $t \to bW^+$ mode are strongly suppressed. Unless the quark–mixing-matrix element $|V_{tb}| \ll 1$, which could occur if top had a strong coupling to a fourth-generation $b'$ with $m_{b'} > m_t$, the decays $t \to (s,d)W^+$ should be extremely rare.[35] It is important to test this expectation by looking for the rare decays directly, or by comparing the number of observed (0, 1, and 2) $b$-tags in a top-quark sample with expectations derived from the various top-production mechanisms and the efficiency for $b$-tagging. The CDF Collaboration has used the tagging method to show that $t \to bW$ accounts for $99 \pm 29\%$ of all $t \to W +$ anything decays.[36]

Stelzer and Willenbrock have argued recently that the $W^\star \to t\bar{b}$ process may in time provide the best measurement of the quark mixing-matrix element $|V_{tb}|$.[37] Prospects for extracting top-quark (and other) parameters from

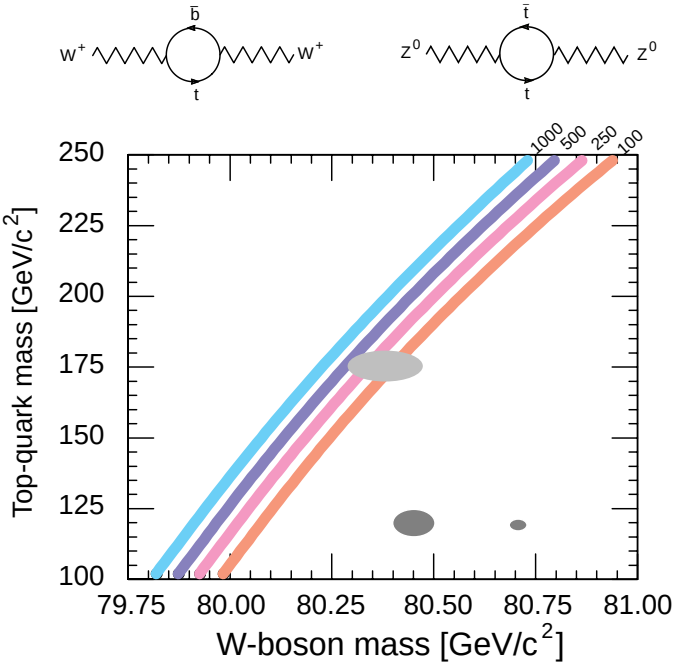


Figure 12: Correlation between the top-quark mass and the $W$-boson mass in the standard electroweak theory. From left to right, the bands correspond to Higgs-boson masses of 1000, 500, 250, and 100 GeV/$c^2$. The thickness of the bands expresses the effect of plausible variations in the value of $\alpha(M_Z)$. The dark region is the one-standard-deviation error ellipse from the current world averages, $m_t = 175.5 \pm 5.1$ GeV/$c^2$ and $M_W = 80.38 \pm 0.09$ GeV/$c^2$. Also shown are the one-standard-deviation error ellipses for precisions expected in the future: ($\delta M_W = 50$ MeV/$c^2$, $\delta m_t = 5$ GeV/$c^2$) and ($\delta M_W = 20$ MeV/$c^2$, $\delta m_t = 2$ GeV/$c^2$). Examples of the heavy-quark loops that give rise to $\Delta\rho$ are shown at the top of the figure.

threshold studies at a future $e^+e^-$ linear collider have been surveyed by Fujii, Matsui, and Sumino.[38]

The rapid decay of the top quark means that there is no time for the formation of top mesons or baryons. Accordingly, the spin orientation of the top quark at the moment of its production is reflected, without dilution, in the decay angular distribution of its decay products. The lepton angular distribution thus becomes a tool for probing the structure of the charged-current interactions of top.[39]

The persistence of the top quark's polarization can be exploited to devise tests for *CP* violation in top decays. Because the standard model leads to very tiny effects, the top system has great sensitivity to nonstandard sources of *CP* violation. A brief review of the considerable literature on the subject can be found in Ref. [40].

The branching ratios expected for the flavor-changing neutral-current decays

$$t \to \begin{pmatrix} g \\ Z \\ \gamma \end{pmatrix} + \begin{pmatrix} c \\ u \end{pmatrix} \tag{56}$$

all are unobservably small ($\ll 10^{-10}$) according to the standard electroweak theory.[41] Anomalous $Zt\bar{c}$ couplings could lead to a branching fraction as large as a few per cent while respecting current constraints from low-energy phenomenology. High-luminosity experiments at the Tevatron or the LHC should be able to explore branching fractions as small as $\sim 10^{-2}$ and $\sim 10^{-4}$, respectively.[42]

Mahlon and Parke have examined the possibility that a threshold enhancement might render observable rare decays like $t \to bWZ$ and $t \to bWH$.[43] The finite widths of the $W$ and $Z$ bosons do raise the decay rates dramatically near threshold, but the branching fractions remain too small to be observed in the current round of experiments. Over the interval 160 GeV/$c^2 \lesssim m_t \lesssim$ 200 GeV/$c^2$, the branching fraction $\Gamma(t \to bWZ)/\Gamma(t \to bW)$ rises from $1.6 \times 10^{-7}$ to $1.4 \times 10^{-5}$. Detection of this mode in a modest top sample would therefore be a compelling sign of new physics.

Because top is so massive, many decay channels may be open to it, beyond the dominant $t \to bW^+$ mode. The semiweak decay $t \to bP^+$, where $P^+$ is a charged (pseudo)scalar, may occur in multi-Higgs generalizations of the standard model, in supersymmetric models, and in technicolor models. The decay rate $\Gamma(t \to bP^+)$ is generically comparable with $\Gamma(t \to bW^+)$, because both are semiweak.[44] An inferred $t\bar{t}$ production cross section smaller than that predicted by QCD would be a hint that $\Gamma(t \to bW^+)/\Gamma(t \to \text{all}) < 1$, which would argue for the presence of nonstandard decays.

Decay of a charged scalar into fermion pairs would typically proceed at a rate

$$\Gamma(P^+ \to f_i \bar{f}_j) = \frac{G_F p (m_i^2 + m_j^2)}{16\pi} C_{ij}, \tag{57}$$

where $p$ is the momentum of the products in the rest frame of $P^+$ and $C_{ij} = (3, 1)$ for (quarks, leptons). The lifetime of $P^+$ is far too short for it to be observed as a short track: for $M_{P^+} = M_W$, $\tau_{P^+} \lesssim 10^{-21}$ s (= 1 zeptosecond).[45] $P^+$ might be reconstructed from its decays into $c\bar{b}$ or $c\bar{s}$, or its presence might be deduced from $P^+ \to \tau^+ \nu_\tau$ decays, which would also lead to violations of lepton universality.

The general lesson is that top decays have the potential to surprise. It may therefore be quite rewarding to learn to tag top-bearing events with high efficiency.[46]

## 11 The Dead Cone

The large mass of the top quark has an important effect on the pattern of soft-gluon emission from an energetic top. If the energy $\omega$ of the gluon is small compared to the energy $E_Q$ of the heavy quark, $\omega \ll E_Q$, then for a gluon emitted at a small angle $\theta \ll 1$ to the top-quark direction, the angular distribution of the radiation will be

$$d\sigma_{Q \to Qg} \sim \frac{\theta^2 d\theta^2}{(\theta^2 + \theta_0^2)^2} \frac{d\omega}{\omega}, \tag{58}$$

where $\theta_0 = m_Q / E_Q$. For angles larger than the critical value, *i.e.*, for $\theta > \theta_0$, the radiation pattern becomes

$$d\sigma \sim \frac{d\theta^2}{\theta^2} \frac{d\omega}{\omega} \to d(\ln \theta^2) d(\ln \omega), \tag{59}$$

which is doubly logarithmic. Indeed, when $\theta \gg \theta_0$, the emission of successive gluons follows a strict angular ordering, and the multiplicity of hadrons accompanying the heavy quark is the same as it would be for a light quark. In contrast, in the very forward cone defined by $\theta < \theta_0$, there is only a single logarithmic factor, $d\omega/\omega$. In this region, gluon emission is inhibited and the multiplicity of accompanying hadrons is diminished. The regime of reduced multiplicity is known as the dead cone.[47]

Although the angular dependence of radiation accompanying a heavy quark has not been measured, there is some evidence for a reduced multiplicity in the number of hadrons emitted by an energetic $b$-quark. The SLD and OPAL

experiments have used tagged samples of $e^+e^- \to Z^0 \to b\bar{b}$ events to compare the charged multiplicity $\langle n_b \rangle$ of hadrons produced by energetic $b$-quarks with the multiplicity $\langle n_{u,d,s} \rangle$ produced by energetic light quarks.[48] SLD finds $\langle n_{u,d,s} \rangle - \langle n_b \rangle = 3.31 \pm 0.41 \pm 0.79$, while OPAL measures $\langle n_{u,d,s} \rangle - \langle n_b \rangle = 3.02 \pm 0.05 \pm 0.79$. This is a significant suppression of particle emission, and bodes well for the possibility of reconstructing self-tagging $B^{**} \to B^{(*)}\pi$ decays cleanly for studies of $CP$ violation in $B$ decays. The effect should be considerably larger for top quarks, which will have the added advantage of decaying before they can be dressed into resonances whose effects are not included in the perturbative analysis.

## 12 Top Matters

It is popular to say that top quarks were produced in great numbers in the fiery cauldron of the Big Bang some fifteen billion years ago, disintegrated in the merest fraction of a second, and vanished from the scene until my colleagues learned to create them in the Tevatron. That would be reason enough to care about top: to learn how it helped sow the seeds for the primordial universe that evolved into our world of diversity and change. But it is not the whole story; it invests the top quark with a remoteness that veils its importance for the everyday world.

The real wonder is that here and now, every minute of every day, the top quark affects the world around us. Through the uncertainty principle of quantum mechanics, top quarks and antiquarks wink in and out of an ephemeral presence in our world. Though they appear virtually, fleetingly, on borrowed time, top quarks have real effects.

Quantum effects make the coupling strengths of the fundamental interactions—appropriately normalized analogues of the fine-structure constant $\alpha$—vary with the energy scale on which the coupling is measured. The fine-structure constant itself has the familiar value 1/137 in the low-energy (or long-wavelength) limit, but grows to about 1/129 at the mass of the $Z^0$ boson, about 91 GeV/$c^2$. Vacuum-polarization effects make the effective electric charge increase at short distances or high energies.

In unified theories of the strong, weak, and electromagnetic interactions, all the coupling "constants" take on a common value, $\alpha_U$, at some high energy, $M_U$. If we adopt the point of view that $\alpha_U$ is fixed at the unification scale, then the mass of the top quark is encoded in the value of the strong coupling $\alpha_s$ that we experience at low energies.[49] Assuming three generations of quarks and leptons, we evolve $\alpha_s$ downwards in energy from the unification scale in the spirit of Georgi, Quinn, and Weinberg.[50] The leading-logarithmic behavior

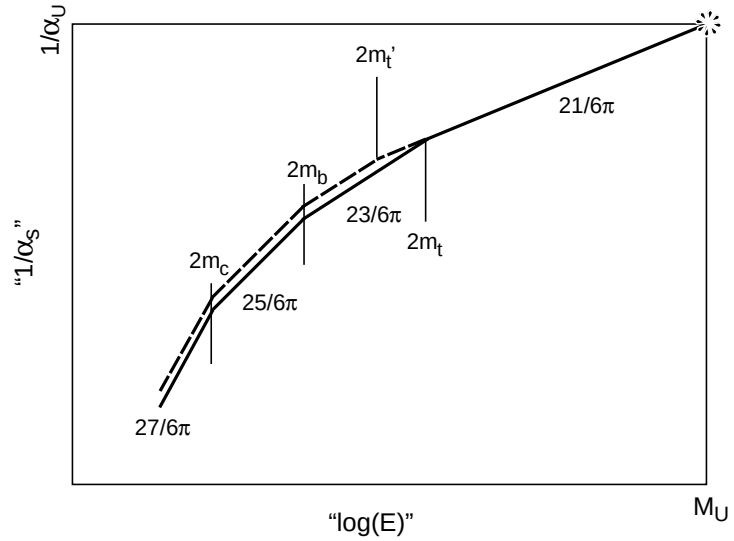


Figure 13: Two evolutions of the strong coupling constant $\alpha_s$. A smaller value of the top-quark mass leads to a smaller value of $\alpha_s$.

is given by

$$1/\alpha_s(Q) = 1/\alpha_U + \tfrac{21}{6\pi} \ln(Q/M_U) \ , \tag{60}$$

for $M_U > Q > 2m_t$. The positive coefficient $+21/6\pi$ means that the strong coupling constant $\alpha_s$ is smaller at high energies than at low energies. This behavior—opposite to the familiar behavior of the electric charge—is the celebrated property of asymptotic freedom. In the interval between $2m_t$ and $2m_b$, the slope $(33-2n_f)/6\pi$ (where $n_f$ is the number of active quark flavors) steepens to $23/6\pi$, and then increases by another $2/6\pi$ at every quark threshold. At the boundary $Q = Q_n$ between effective field theories with $n-1$ and $n$ active flavors, the coupling constants $\alpha_s^{(n-1)}(Q_n)$ and $\alpha_s^{(n)}(Q_n)$ must match. This behavior is shown by the solid line in Figure 13.

The dotted line in Figure 13 shows how the evolution of $1/\alpha_s$ changes if the top-quark mass is reduced. A smaller top mass means a larger low-energy value of $1/\alpha_s$, so a smaller value of $\alpha_s$.

Neglecting the tiny "current-quark" masses of the up and down quarks, the scale parameter $\Lambda_{\rm QCD}$ is the only mass parameter in QCD. It determines the scale of the confinement energy that is the dominant contribution to the proton mass. To a good first approximation,

$$M_{\rm proton} \approx C\Lambda_{\rm QCD}, \tag{61}$$

where the constant of proportionality $C$ is calculable using techniques of lattice field theory.

To discover the dependence of $\Lambda_{\rm QCD}$ upon the top-quark mass, we calculate $\alpha_s(2m_t)$ evolving up from low energies and down from the unification scale, and match:

$$1/\alpha_U + \tfrac{21}{6\pi}\ln(2m_t/M_U) = 1/\alpha_s(2m_c) - \tfrac{25}{6\pi}\ln(m_c/m_b) - \tfrac{23}{6\pi}\ln(m_b/m_t). \quad (62)$$

Identifying

$$1/\alpha_s(2m_c) \equiv \tfrac{27}{6\pi}\ln(2m_c/\Lambda_{\rm QCD}) \ , \quad (63)$$

we find that

$$\Lambda_{\rm QCD} = e^{-6\pi/27\alpha_U}\left(\frac{M_U}{1\ {\rm GeV}}\right)^{21/27}\left(\frac{2m_t\cdot 2m_b\cdot 2m_c}{1\ {\rm GeV}^3}\right)^{2/27}\ {\rm GeV}\ . \quad (64)$$

We conclude that, in a simple unified theory,

$$\frac{M_{\rm proton}}{1\ {\rm GeV}} \propto \left(\frac{m_t}{1\ {\rm GeV}}\right)^{2/27} \ , \quad (65)$$

so that, for example, a factor-of-ten decrease in the top-quark mass would result in a 20% decrease in the proton mass. This is a wonderful result. Now, we can't use it to compute the mass of the top quark, because we don't know the values of $M_U$ and $\alpha_U$, and haven't yet calculated precisely the constant of proportionality between the proton mass and the QCD scale parameter. Never mind! The important lesson—no surprise to any twentieth-century physicist—is that the microworld does determine the behavior of the quotidian. We will fully understand the origin of one of the most important parameters in the everyday world—the mass of the proton—only by knowing the properties of the top quark.[51]

Top matters!

## 13 Top's Yukawa Coupling

In the $SU(2)_L \otimes U(1)_Y$ electroweak theory, Higgs scalars give masses to the electroweak gauge bosons $W^\pm$ and $Z^0$, and also to the elementary fermions. While the gauge-boson masses are determined in terms of the weak mixing parameter $\sin^2\theta_W$, each fermion mass is set by a distinct Yukawa coupling, as

$$m_f = \frac{G_f v}{\sqrt{2}}, \quad (66)$$

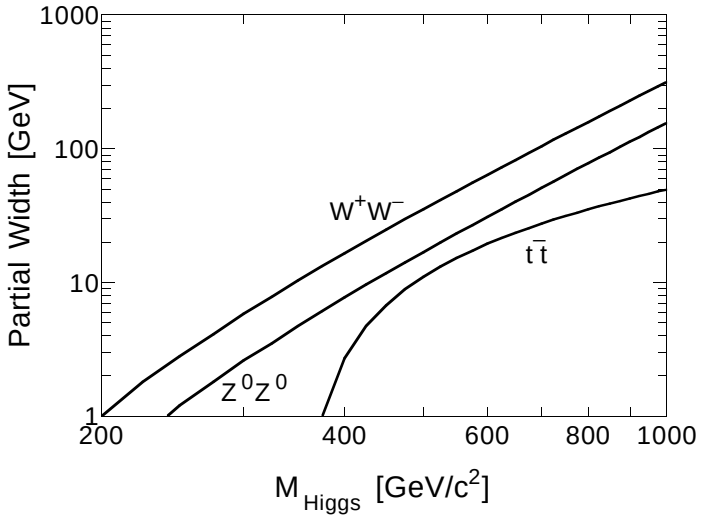


Figure 14: Partial widths for the prominent decay modes of a heavy Higgs boson.

where $v = (G_F\sqrt{2})^{-1/2} \approx 246$ GeV. The Yukawa coupling of the electron is $G_e \approx 3 \times 10^{-6}$.

The top quark stands apart from the other fundamental constituents because its Yukawa coupling is very close to unity: $G_t \approx 1$. Is top special? Or is it the only normal fermion?

In either case, the large $Ht\bar{t}$ coupling has several implications. (i) Higgs interactions will exert a significant influence on the evolution of the top-quark mass. As we examine the possibility that the pattern of fermion masses is more intelligible at the unification scale than at the scale of common experience, it is important to evolve the fermion masses to our scale with care.[52] (ii) It is worth reexamining the reactions $q\bar{q} \to (\gamma^\star, Z^\star) \to t\bar{t}H$ and $q\bar{q} \to Z^\star \to ZH \to Zt\bar{t}$ at the LHC or, with $e^+e^-$ replacing $q\bar{q}$, at a multi-TeV linear collider. (iii) A heavier top quark is a more important product of heavy-Higgs decay. Figure 14 shows the partial widths for Higgs-boson decay into the dominant $W^+W^-$ and $Z^0Z^0$ channels and into $t\bar{t}$, for $m_t = 175$ GeV/$c^2$. Whether the $t\bar{t}$ mode will be useful to confirm the observation of the Higgs boson, or merely drains probability from the favored $ZZ$ channel, is a question for detailed detector simulations.

## 14 Are We Luckier Than We Deserve?

According to the cockroach theory of stock market analysis, there is never a single piece of good news or bad news. Might the discovery of top be the precursor of other discoveries? More specifically, might the signal attributed to top also contain evidence of other new particles? Let us review two possibilities.

A heavy top influences the spectrum analysis in minimal supersymmetric extensions of the standard model. In some supersymmetric models, the lighter of the top squark eigenstates, called $\tilde{t}_1$, is less massive than the top quark: $m_{\tilde{t}_1} < m_t$.[53] Typically, the cross section for production of a heavy squark pair in $q\bar{q}$ interactions is about 1/8 to 1/4 of the cross section for production of a pair of quarks of the same mass. Consequently, production of $\tilde{t}_1\tilde{t}_1^*$ is unlikely to distort the "top" production cross section dramatically. If it is kinematically allowed, the chain

$$\begin{aligned} \tilde{t}_1 \quad &\to \quad b\widetilde{W}^+ \\ &\qquad \hookrightarrow W^+\tilde{\chi}^0 \\ &\qquad\quad \hookrightarrow \ell\nu \ , \end{aligned} \tag{67}$$

where $\widetilde{W}^+$ is a wino and $\tilde{\chi}^0$ a neutralino, should be prominent among many decay channels. It is a challenge to devise search strategies for the top squark and its decay products.

A second new quark, nearly degenerate with top, would have a stronger influence on "$\sigma(t\bar{t})$." Barger and Phillips [54] have explored the consequences of a weak-isoscalar, charge-2/3 quark, $t_s$, close in mass to top. This singlet quark would decay by mixing with top ($t_s \to t \to bW^+$), so would populate the same decay modes. By choosing $m_{t_s} \approx m_t$, it is easy to double the apparent top cross section. Given the close agreement between measured and calculated cross sections for top production, we do not currently have a phenomenological incentive to do this. However, the questions raised by this scenario are important and of general interest: Is the reconstructed top-quark mass distribution normal? Is the $t\bar{t}$ effective-mass distribution normal? Some numerical examples have been studied by Lane.[55]

## 15 Resonances in $t\bar{t}$ Production?

Because objects associated with the breaking of electroweak symmetry tend to couple to fermion mass, the discovery of top opens a new window on electroweak symmetry breaking. The possibility of new sources of $t\bar{t}$ pairs makes it urgent to test how closely top production conforms to standard (QCD) expectations.

Two classes of models have received considerable attention in the context of a heavy top quark. Top-condensate models and multiscale technicolor both imply the existence of color-octet resonances that decay into $t\bar{t}$, for which the natural mass scale is a few hundred GeV/$c^2$. We are led to ask: Is there a resonance in $t\bar{t}$ production? How is it made? How (else) does it decay?

In the standard Higgs model of electroweak symmetry breaking, the Higgs potential breaks the $SU(2)_L \otimes U(1)_Y$ gauge symmetry. The nonzero vacuum expectation value of the Higgs field endows the $W^{\pm}$ and $Z^0$ with mass and, through the arbitrary Yukawa couplings of the Higgs field to fermions, gives masses to the quarks and leptons. The Higgs mechanism is a relativistic generalization of the Ginzburg–Landau phenomenology of the superconducting phase transition. Both technicolor and topcolor are dynamical symmetry breaking schemes that are inspired by the Bardeen–Cooper–Schrieffer theory of superconductivity.

In technicolor, the QCD-like technicolor interaction becomes strong at low energies and forms a technifermion condensate that breaks chiral symmetry and gives masses to the gauge bosons $W^{\pm}$ and $Z^0$. In a generalization of the basic scheme known as extended technicolor, new gauge bosons couple ordinary fermions to technifermions and allow the fermions to communicate with the technifermion condensate and acquire mass.[56] In topcolor, a new interaction drives the formation of a $\langle \bar{t}t \rangle$ condensate that hides the electroweak symmetry and gives masses to the ordinary fermions.[57]

In the technicolor picture, which has been elaborated recently by Eichten and Lane,[58] a color-octet analogue of the $\eta'$ meson, called $\eta_T$, is produced in gluon-gluon interactions. The sequence

$$gg \to \eta_T \to (gg, t\bar{t}) \tag{68}$$

leads to distortions of the $t\bar{t}$ invariant-mass distribution, and of the two-jet invariant-mass distribution. Since $\Gamma(\eta_T \to b\bar{b})/\Gamma(\eta_T \to t\bar{t}) = m_b^2/m_t^2$, there should be only a negligible perturbation on the $b\bar{b}$ invariant-mass distribution.

In the topcolor picture explored by Hill and Parke,[59] a massive vector "coloron" can be produced in $q\bar{q}$ interactions. The coloron decays at comparable rates into $t\bar{t}$ and $b\bar{b}$ and can appear as a resonance peak in both channels. There is no clear reason to expect the coloron to distort the untagged two-jet invariant-mass spectrum.

If an enhancement were to be seen in the $t\bar{t}$ channel, a useful differential diagnostic, in addition to the $b\bar{b}$ and jet-jet invariant-mass distributions, will be the $t\bar{t}$ mass spectrum in different rapidity intervals and at different energies. It is useful to recall from our discussion of top production rates in §6 that the relative $gg$ and $q\bar{q}$ luminosities at high masses change significantly between $\bar{p}p$

energies of 1.8 and 2.0 TeV. At the LHC, the large $gg$ luminosity would greatly enhance the contribution of $\eta_T$ with respect to the standard QCD process. The isotropic decays of $\eta_T$ will help to characterize the technicolor case. Hill and Parke [59] and Lane [55] have investigated the discriminatory power of $d\sigma/dp_\perp$ and of the production angular distributions for top.

When searching for resonances and other exotic sources of top, it is important not to apply cuts that efficiently exclude all mechanisms but standard QCD production. Traditional expectations for sphericity, aplanarity, and similar event-shape parameters may not be realized for new sources.

## 16 Hiding a Gauge Symmetry

The most apt analogy for the hiding of the electroweak gauge symmetry is found in superconductivity. In the Ginzburg-Landau description [60] of the superconducting phase transition, a superconducting material is regarded as a collection of two kinds of charge carriers: normal, resistive carriers, and superconducting, resistanceless carriers.

In the absence of a magnetic field, the free energy of the superconductor is related to the free energy in the normal state through

$$G_{\rm super}(0) = G_{\rm normal}(0) + \alpha\,|\psi|^2 + \beta\,|\phi|^4 \quad , \tag{69}$$

where $\alpha$ and $\beta$ are phenomenological parameters and $|\psi|^2$ is an order parameter corresponding to the density of superconducting charge carriers. The parameter $\beta$ is non-negative, so that the free energy is bounded from below.

Above the critical temperature for the onset of superconductivity, the parameter $\alpha$ is positive and the free energy of the substance is supposed to be an increasing function of the density of superconducting carriers, as shown in Figure 15(a). The state of minimum energy, the vacuum state, then corresponds to a purely resistive flow, with no superconducting carriers active. Below the critical temperature, $\alpha$ is negative and the free energy is minimized when $\psi = \psi_0 \neq 0$, as illustrated in Figure 15(b).

This is a nice cartoon description of the superconducting phase transition, but there is more. In an applied magnetic field $\vec{H}$, the free energy is

$$G_{\rm super}(\vec{H}) = G_{\rm super}(0) + \frac{\vec{H}^2}{8\pi} + \frac{1}{2m^\star}|-i\hbar\nabla\psi - (e^\star/c)\vec{A}\psi|^2 \quad , \tag{70}$$

where $e^\star$ and $m^\star$ are the charge ($-2$ units) and effective mass of the superconducting carriers. In a weak, slowly varying field $\vec{H} \approx 0$, when we can

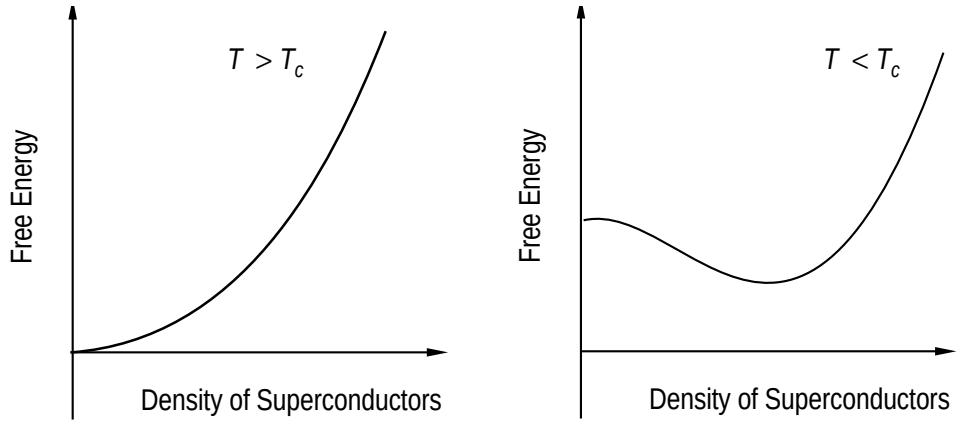


Figure 15: Ginzburg-Landau description of the superconducting phase transition.

approximate $\psi \approx \psi_0$ and $\nabla\psi \approx 0$, the usual variational analysis leads to the equation of motion,

$$\nabla^2 \vec{A} - \frac{4\pi e^\star}{m^\star c^2} \left|\psi_0\right|^2 \vec{A} = 0 \ , \tag{71}$$

the wave equation of a massive photon. In other words, the photon acquires a mass within the superconductor. This is the origin of the Meissner effect, the exclusion of a magnetic field from a superconductor. More to the point, for our purposes, it shows how a symmetry-hiding phase transition can lead to a massive gauge boson.

To give masses to the intermediate bosons of the weak interaction, we take advantage of a relativistic generalization of the Ginzburg-Landau phase transition known as the Higgs mechanism.[61] We introduce auxiliary scalar fields, with gauge-invariant interactions among themselves and with the fermions and bosons of the electroweak theory. We then arrange their self-interactions so that the vacuum state corresponds to a broken-symmetry solution. As a result, the $W$ and $Z$ bosons acquire masses, as auxiliary scalars assume the role of the third (longitudinal) degrees of freedom of what had been massless gauge bosons. The quarks and leptons acquire masses as well, from their Yukawa interactions with the scalars. Finally, there remains as a vestige of the spontaneous breaking of the symmetry a massive, spin-zero particle, the Higgs boson. Though what we take to be the work of the Higgs boson is all around us, the Higgs particle itself has not yet been observed.

It is remarkable that the resulting theory has been tested at distances rang-

ing from about $10^{-17}$ cm to about $4\times10^{20}$ cm, especially when we consider that classical electrodynamics has its roots in the tabletop experiments that gave us Coulomb's law. These basic ideas were modified in response to the quantum effects observed in atomic experiments. High-energy physics experiments both inspired and tested the unification of weak and electromagnetic interactions. At distances longer than common experience, electrodynamics—in the form of the statement that the photon is massless—has been tested in measurements of the magnetic fields of the planets. With additional assumptions, the observed stability of the Magellanic clouds provides evidence that the photon is massless over distances of about $10^{22}$ cm.

## 17 A Higgs Boson Must Exist

How can we be sure that a Higgs boson, or something very like it, will be found? One path to the *theoretical* discovery of the Higgs boson involves its role in the cancellation of high-energy divergences. An illuminating example is provided by the reaction

$$e^+e^- \to W^+W^-, \tag{72}$$

which is described in lowest order by the four Feynman graphs in Figure 16. The contributions of the direct-channel $\gamma$- and $Z^0$-exchange diagrams of Figs. 16(a) and (b) cancel the leading divergence in the $J = 1$ partial-wave amplitude of the neutrino-exchange diagram in Figure 16(c). However, the $J = 0$ partial-wave amplitude, which exists in this case because the electrons are massive and may therefore be found in the "wrong" helicity state, grows as $s^{1/2}$ for the production of longitudinally polarized gauge bosons. The resulting divergence is precisely cancelled by the Higgs boson graph of Figure 16(d). If the Higgs boson did not exist, something else would have to play this role. From the point of view of $S$-matrix analysis, the Higgs-electron-electron coupling must be proportional to the electron mass, because "wrong-helicity" amplitudes are always proportional to the fermion mass.

Let us underline this result. If the gauge symmetry were unbroken, there would be no Higgs boson, no longitudinal gauge bosons, and no extreme divergence difficulties. But there would be no viable low-energy phenomenology of the weak interactions. The most severe divergences of individual diagrams are eliminated by the gauge structure of the couplings among gauge bosons and leptons. A lesser, but still potentially fatal, divergence arises because the electron has acquired mass—because of the Higgs mechanism. Spontaneous symmetry breaking provides its own cure by supplying a Higgs boson to re-

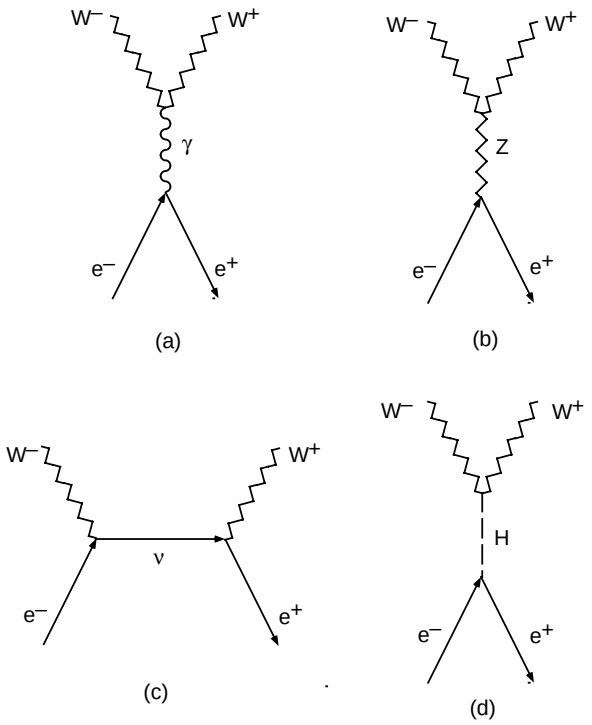


Figure 16: Lowest-order contributions to the $e^+e^- \to W^+W^-$ scattering amplitude.

move the last divergence. A similar interplay and compensation must exist in any satisfactory theory.

> **Problem:** Carry out the computation of the amplitudes for the reaction $e^+e^- \to W^+W^-$ described above, retaining the electron mass. Verify the role of the Higgs boson in the cancellation of divergences. (*Nota bene:* If you do only one gauge-theory calculation in your life, this should be the one!)

## 18 Why is the Electroweak Scale Small?

The $SU(2)_L \otimes U(1)_Y$ electroweak theory does not explain how the scale of electroweak symmetry breaking is maintained in the presence of quantum corrections. The problem of the scalar sector can be summarized neatly as follows.[62]

The Higgs potential is

$$V(\phi^\dagger\phi) = \mu^2(\phi^\dagger\phi) + |\lambda|\,(\phi^\dagger\phi)^2 \ . \tag{73}$$

With $\mu^2$ chosen to be less than zero, the electroweak symmetry is spontaneously broken down to the $U(1)$ of electromagnetism, as the scalar field acquires a vacuum expectation value that is fixed by the low-energy phenomenology,

$$\langle\phi\rangle_0 = \sqrt{-\mu^2/2|\lambda|} \equiv (G_F\sqrt{8})^{-1/2} \approx 175 \text{ GeV} \ . \tag{74}$$

Beyond the classical approximation, scalar mass parameters receive quantum corrections from loops that contain particles of spins $J = 1, 1/2$, and 0:

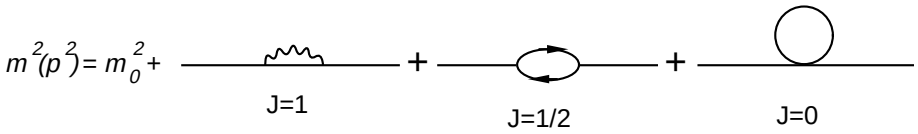


(75)

The loop integrals are potentially divergent. Symbolically, we may summarize the content of (75) as

$$m^2(p^2) = m^2(\Lambda^2) + Cg^2\int_{p^2}^{\Lambda^2} dk^2 + \cdots \ , \tag{76}$$

where $\Lambda$ defines a reference scale at which the value of $m^2$ is known, $g$ is the coupling constant of the theory, and the coefficient $C$ is calculable in any particular theory. Instead of dealing with the relationship between observables and parameters of the Lagrangian, we choose to describe the variation of an observable with the momentum scale. In order for the mass shifts induced by radiative corrections to remain under control (*i.e.*, not to greatly exceed the value measured on the laboratory scale), either

- $\Lambda$ must be small, so the range of integration is not enormous, or
- new physics must intervene to cut off the integral.

If the fundamental interactions are described by an $SU(3)_c \otimes SU(2)_L \otimes U(1)_Y$ gauge symmetry, *i.e.*, by quantum chromodynamics and the electroweak theory, then the natural reference scale is the Planck mass,

$$\Lambda \sim M_{\rm Planck} \approx 10^{19} \text{ GeV} \ . \tag{77}$$

In a unified theory of the strong, weak, and electromagnetic interactions, the natural scale is the unification scale,

$$\Lambda \sim M_U \approx 10^{15}\text{-}10^{16}\ \text{GeV} \ . \tag{78}$$

Both estimates are very large compared to the scale of electroweak symmetry breaking (74). We are therefore assured that new physics must intervene at an energy of approximately 1 TeV, in order that the shifts in $m^2$ not be much larger than (74).

Only a few distinct scenarios for controlling the contribution of the integral in (76) can be envisaged. The supersymmetric solution is especially elegant. Exploiting the fact that fermion loops contribute with an overall minus sign (because of Fermi statistics), supersymmetry balances the contributions of fermion and boson loops. In the limit of unbroken supersymmetry, in which the masses of bosons are degenerate with those of their fermion counterparts, the cancellation is exact:

$$\sum_{i=\substack{\text{fermions}\\+\text{bosons}}} C_i \int dk^2 = 0 \ . \tag{79}$$

If the supersymmetry is broken (as it must be in our world), the contribution of the integrals may still be acceptably small if the fermion-boson mass splittings $\Delta M$ are not too large. The condition that $g^2 \Delta M^2$ be "small enough" leads to the requirement that superpartner masses be less than about 1 TeV/$c^2$.

A second solution to the problem of the enormous range of integration in (76) is offered by theories of dynamical symmetry breaking such as technicolor. In technicolor models, the Higgs boson is composite, and new physics arises on the scale of its binding, $\Lambda_{TC} \simeq O(1\ \text{TeV})$. Thus the effective range of integration is cut off, and mass shifts are under control.

A third possibility is that the gauge sector becomes strongly interacting. This would give rise to $WW$ resonances, multiple production of gauge bosons, and other new phenomena at energies of 1 TeV or so. It is likely that a scalar bound state—a quasi-Higgs boson—would emerge with a mass less than about 1 TeV/$c^2$.

We cannot avoid the conclusion that some new physics must occur on the 1-TeV scale.

## 19 Triviality of Scalar Field Theory

The electroweak theory itself provides another reason to expect that discoveries will not end with the Higgs boson. Scalar field theories make sense on all

energy scales only if they are noninteracting, or "trivial."[63] The vacuum of quantum field theory is a dielectric medium that screens charge. Accordingly, the effective charge is a function of the distance or, equivalently, of the energy scale. This is the famous phenomenon of the running coupling constant.

In $\lambda\phi^4$ theory (compare the interaction term in the Higgs potential), it is easy to calculate the variation of the coupling constant $\lambda$ in perturbation theory by summing bubble graphs like this one:

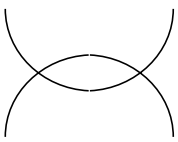

. (80)

The coupling constant $\lambda(\mu)$ on a physical scale $\mu$ is related to the coupling constant on a higher scale $\Lambda$ by

$$\frac{1}{\lambda(\mu)} = \frac{1}{\lambda(\Lambda)} + \frac{3}{2\pi^2}\log\left(\Lambda/\mu\right) \ . \tag{81}$$

This perturbation-theory result is reliable only when $\lambda$ is small, but lattice field theory allows us to treat the strong-coupling regime.

In order for the Higgs potential to be stable (*i.e.*, for the energy of the vacuum state not to race off to $-\infty$), $\lambda(\Lambda)$ must not be negative. Therefore we can rewrite (81) as an inequality,

$$\frac{1}{\lambda(\mu)} \geq \frac{3}{2\pi^2}\log\left(\Lambda/\mu\right) \ . \tag{82}$$

This gives us an *upper bound*,

$$\lambda(\mu) \leq 2\pi^2/3\log\left(\Lambda/\mu\right) \ , \tag{83}$$

on the coupling strength at the physical scale $\mu$. If we require the theory to make sense to arbitrarily high energies—or short distances—then we must take the limit $\Lambda \to \infty$ while holding $\mu$ fixed at some reasonable physical scale. In this limit, the bound (83) forces $\lambda(\mu)$ to zero. The scalar field theory has become free field theory; in theorist's jargon, it is trivial.

We can rewrite the inequality (83) as a bound on the Higgs-boson mass. Rearranging and exponentiating both sides gives the condition

$$\Lambda \leq \mu \exp\left(\frac{2\pi^2}{3\lambda(\mu)}\right) \ . \tag{84}$$

Choosing the physical scale as $\mu = M_H$, and remembering that, before quantum corrections,

$$M_H^2 = 2\lambda(M_H)v^2 \ , \tag{85}$$

where $v = (G_F\sqrt{2})^{-1/2} \approx 246$ GeV is the vacuum expectation value of the Higgs field times $\sqrt{2}$, we find that

$$\Lambda \leq M_H \exp\left(\frac{4\pi^2 v^2}{3M_H^2}\right) \ . \tag{86}$$

For any given Higgs-boson mass, there is a maximum energy scale $\Lambda^\star$ at which the theory ceases to make sense. The description of the Higgs boson as an elementary scalar is at best an effective theory, valid over a finite range of energies.

If the Higgs boson is relatively light—which would itself require explanation—then the theory can be self-consistent up to very high energies. If the electroweak theory is to make sense all the way up to a unification scale $\Lambda^\star = 10^{16}$ GeV, then the Higgs boson must weigh less than 170 GeV/$c^2$.[64]

This perturbative analysis breaks down when the Higgs-boson mass approaches 1 TeV/$c^2$ and the interactions become strong. Lattice analyses [65] indicate that, for the theory to make sense up to a few TeV, the mass of the Higgs boson can be no more than about 800 GeV/$c^2$. Another way of putting this result is that, if the elementary Higgs boson takes on the largest mass allowed by perturbative unitarity arguments, the electroweak theory will be living on the brink of instability.

## 20 New Physics Nearby

### *20.1 Supersymmetry*

Since we have profited in Maó from Gian Giudice's excellent lecture series on supersymmetric models, I will content myself with a few general remarks about the motivation for supersymmetry on the electroweak scale, and its connection with string theory.[66]

One of the best phenomenological motivations for supersymmetry on the 1-TeV scale is that the minimal supersymmetric extension of the standard model so closely approximates the standard model itself. This is a nontrivial property of new physics beyond the standard model, and a requirement urged on us by the unbroken quantitative success of the established theory. On the aesthetic—or theoretical—side, supersymmetry is the maximal—indeed, unique—extension of Poincaré invariance. It also offers a path to the incorporation of gravity, since local supersymmetry leads directly to supergravity. As

a practical matter, supersymmetry on the 1-TeV scale offers a solution to the naturalness problem, and allows a fundamental scalar to exist at low energies.

When we combine supersymmetry with unification of the fundamental forces, we obtain a satisfactory prediction for the weak mixing parameter, $\sin^2\theta_W$, and a simple picture of coupling-constant unification. Adding an assumption of universality, we are led naturally to a picture in which the top mass is linked with the electroweak scale, so that $m_t \approx v/\sqrt{2}$. Finally, the assumption of $R$-parity leads to a stable lightest supersymmetric particle, which is a natural candidate for the dark matter of the Universe.

Supersymmetry doubles the spectrum of fundamental particles. We know that supersymmetry must be significantly broken in Nature, because the electron is manifestly not degenerate in mass with its scalar partner, the selectron. It is interesting to contemplate just how different the world would have been if the selectron, not the electron, were the lightest charged particle and therefore the stable basis of everyday matter.[51] If atoms were selectronic, there would be no Pauli principle to dictate the integrity of molecules. As Dyson [67] and Lieb [68] demonstrated, transforming electrons and nucleons from fermions to bosons would cause all molecules to shrink into an insatiable undifferentiated blob. Luckily, there is no analogue of chiral symmetry to guarantee naturally small squark and slepton masses. So while supersymmetry menaces us with an amorphous death, it is likely that a full understanding of supersymmetry will enable us to explain why we live in a universe ruled by the exclusion principle.

Many theorists take a step beyond supersymmetry to string theory, the only known consistent theory of quantum gravity.[69] String theory aspires to unite all the fundamental interactions in one (and only one?) theory with few free parameters. If successful, this program might explain the standard-model gauge group, unified extensions to the $SU(3)_c \otimes SU(2)_L \otimes U(1)_Y$ gauge symmetry, and the fermion content of the standard model. String theory makes two generic predictions for physics beyond the standard model: additional $U(1)$ subgroups of the unifying group lead to new gauge bosons, and additional colored fermions augment the spectrum of fundamental constituents.

In spite of what doubters often say, there *is* experimental support for string theory from accelerator experiments. Superstrings predicted gravity in 1974,[70] and LEP accelerator physicists detected tidal forces in 1993.[71] What more empirical evidence could one demand?

### *20.2 Technicolor*

Dynamical symmetry breaking provides a different solution to the naturalness problem of the electroweak theory: in technicolor, there are no elementary

scalars. We hope that solving the dynamics that binds elementary fermions into a composite Higgs boson and other $WW$ resonances will bring addition predictive power. It is worth saying that technicolor is a far more ambitious program than global supersymmetry. It doesn't merely seek to finesse the hierarchy problem, it aims to predict the mass of the Higgs surrogate. Against the aesthetic appeal of supersymmetry we can weigh technicolor's excellent pedigree. As we have seen in §16, the Higgs mechanism of the standard model is the relativistic generalization of the Ginzburg-Landau description of the superconducting phase transition. Dynamical symmetry breaking schemes—technicolor and its relatives—are inspired by the Bardeen–Cooper–Schrieffer theory of superconductivity, and seek to give a similar microscopic description of electroweak symmetry breaking.

In its simplest form, technicolor makes no prediction for fermion masses. Consequently, technicolor serves as a reminder that there are two problems of mass: explaining the masses of the gauge bosons, which demands and understanding of electroweak symmetry breaking; and accouting for the quark and lepton masses, which requires not only an understanding of electroweak symmetry breaking but also a theory of the Yukawa couplings that set the scale of fermion masses in the standard model.

The dynamical-symmetry-breaking approach realized in technicolor theories is modeled upon our understanding of the superconducting phase transition.[72,73] The macroscopic order parameter of the Ginzburg-Landau phenomenology corresponds to the wave function of superconducting charge carriers. As we have seen in §2 and 16, it acquires a nonzero vacuum expectation value in the superconducting state. The microscopic Bardeen-Cooper-Schrieffer theory[74] identifies the dynamical origin of the order parameter with the formation of bound states of elementary fermions, the Cooper pairs of electrons. The basic idea of technicolor is to replace the elementary Higgs boson with a fermion-antifermion bound state. By analogy with the superconducting phase transition, the dynamics of the fundamental technicolor gauge interactions among technifermions generate scalar bound states, and these play the role of the Higgs fields.

The elementary fermions—electrons—and the gauge interactions—QED—needed to generate the scalar bound states are already present in the case of superconductivity. Could a scheme of similar economy account for the transition that hides the electroweak symmetry? Consider an $SU(3)_c \otimes SU(2)_L \otimes U(1)_Y$ theory of massless up and down quarks. Because the strong interaction is strong, and the electroweak interaction is feeble, we may treat the $SU(2)_L \otimes U(1)_Y$ interaction as a perturbation. For vanishing quark masses, QCD has an exact $SU(2)_L \otimes SU(2)_R$ chiral symmetry. At an energy scale $\sim \Lambda_{\rm QCD}$, the

strong interactions become strong, fermion condensates appear, and the chiral symmetry is spontaneously broken to the familiar flavor symmetry:

$$SU(2)_L \otimes SU(2)_R \to SU(2)_V \quad . \tag{87}$$

Three Goldstone bosons appear, one for each broken generator of the original chiral invariance. These were identified by Nambu [75] as three massless pions.

The broken generators are three axial currents whose couplings to pions are measured by the pion decay constant $f_\pi$. When we turn on the $SU(2)_L \otimes U(1)_Y$ electroweak interaction, the electroweak gauge bosons couple to the axial currents and acquire masses of order $\sim g f_\pi$. The massless pions thus disappear from the physical spectrum, having become the longitudinal components of the weak gauge bosons. Unfortunately, the mass acquired by the intermediate bosons is far smaller than required for a successful low-energy phenomenology; it is only [76] $M_W \sim 30$ MeV/$c^2$.

The minimal technicolor model of Weinberg [77] and Susskind [78] transcribes the same ideas from QCD to a new setting. The technicolor gauge group is taken to be $SU(N)_{TC}$ (usually $SU(4)_{TC}$), so the gauge interactions of the theory are generated by

$$SU(4)_{TC} \otimes SU(3)_c \otimes SU(2)_L \otimes U(1)_Y \ . \tag{88}$$

The technifermions are a chiral doublet of massless color singlets

$$\begin{pmatrix} U \\ D \end{pmatrix}_L \quad U_R,\ D_R \ . \tag{89}$$

With the electric charge assignments $Q(U) = \frac{1}{2}$ and $Q(D) = -\frac{1}{2}$, the theory is free of electroweak anomalies. The ordinary fermions are all technicolor singlets.

In analogy with our discussion of chiral symmetry breaking in QCD, we assume that the chiral $TC$ symmetry is broken,

$$SU(2)_L \otimes SU(2)_R \otimes U(1)_V \to SU(2)_V \otimes U(1)_V \ . \tag{90}$$

Three would-be Goldstone bosons emerge. These are the technipions

$$\pi_T^+, \quad \pi_T^0, \quad \pi_T^-, \tag{91}$$

for which we are free to *choose* the technipion decay constant as

$$F_\pi = \left( G_F \sqrt{2} \right)^{-1/2} = 246 \text{ GeV} \ . \tag{92}$$

This amounts to choosing the scale on which technicolor becomes strong. When the electroweak interactions are turned on, the technipions become the longitudinal components of the intermediate bosons, which acquire masses

$$\begin{aligned} M_W^2 &= g^2 F_\pi^2/4 &&= \frac{\pi\alpha}{G_F\sqrt{2}\sin^2\theta_W} \\ M_Z^2 &= \left(g^2+g'^2\right)F_\pi^2/4 &&= M_W^2/\cos^2\theta_W \end{aligned} \tag{93}$$

that have the canonical Standard Model values, thanks to our choice (92) of the technipion decay constant.

Technicolor shows how the generation of intermediate boson masses could arise without fundamental scalars or unnatural adjustments of parameters. It thus provides an elegant solution to the naturalness problem of the Standard Model. However, it has a major deficiency: it offers no explanation for the origin of quark and lepton masses, because no Yukawa couplings are generated between Higgs fields and quarks or leptons.

A possible approach to the problem of quark and lepton masses is suggested by "extended technicolor" models and their modern extensions, "walking technicolor" models.[79] Technicolor implies a number of spinless technipions with masses below the technicolor scale of about 1 TeV. Some of these, the color singlet, technicolor singlet particles, should be relatively light. The colored technipions and technivector mesons may just be accessible to experiments at the Tevatron, but a thorough investigation awaits experiments on the 1-TeV scale.[80]

### *20.3 Implications of Heavy Top*

The great mass of the top quark is suggestive for both the supersymmetry and dynamical symmetry breaking approaches. Within the framework of supersymmetry, the heavy top quark encourages the belief in low-scale supersymmetry, and suggests that the discovery of supersymmetry may be at hand, either at LEP2 or at the Tevatron Collider. To me, the proximity of the top mass to the scale of electroweak symmetry breaking argues that the two problems of mass—mass for the gauge bosons and mass for the fermions—may be one. In other words, the heavy top makes it less likely that the question of flavor can be postponed, and more likely that it is of a piece with the problem of electroweak symmetry breaking. This linkage is (almost) surely true in any dynamical symmetry breaking scheme, and I find it an appealing conclusion in general. Because of the heavy top, I am now optimistic that exploring the 1-TeV scale will illuminate the flavor question as well as electroweak symmetry breaking.

*20.4 New Strong Dynamics*

If new strong dynamics at the 1-TeV scale replaces the elementary Higgs boson of the standard model, then it is reasonable to expect low-energy signals of the new dynamics. There are two interesting options to explore:

- Replace the Higgs sector only with a composite. This is the approach followed in Technicolor and its generalizations to "walking" technicolor or two-scale technicolor, topcolor, and topcolor-assisted technicolor.
- The quarks and leptons are composite, as well as the Higgs boson, on a scale $\Lambda^\star \approx$ a few TeV. The dynamics of a composite model of quarks and leptons is quite unlike that of QCD, for the massless particle of the theory must be the fermions, not the analogues of pions. If quarks and leptons are composite, we might hope to gain an understanding of generations and of fermion masses.

In the following Section, I briefly review what is known—and desired— about composite models of our "elementary" particles, the quarks and leptons.

## 21 Composite Quarks and Leptons?

Throughout these lectures, we have assumed the quarks and leptons to be elementary point particles. This is consistent with the experimental observations to date that the "size" of quarks and leptons is bounded from above by

$$R < 10^{-17} \text{ cm} . \tag{94}$$

Indeed, the identification of quarks and leptons as elementary particles (whether that distinction holds at all distance scales or only the regime we are now able to explore) is an important ingredient in the simplicity of the standard model.

We may nevertheless wish to entertain the possibility that the quarks and leptons are themselves composites of some still more fundamental structureless particles, for the followeing reasons:

- The proliferation of "fundamental" fermions

$$\begin{array}{llll} \begin{pmatrix} u \\ d \end{pmatrix}_L & \begin{pmatrix} c \\ s \end{pmatrix}_L & \begin{pmatrix} t \\ b \end{pmatrix}_L & u_R, d_R, s_R, c_R, b_R, t_R \\ \begin{pmatrix} \nu_e \\ e \end{pmatrix}_L & \begin{pmatrix} \nu_\mu \\ \mu \end{pmatrix}_L & \begin{pmatrix} \nu_\tau \\ \tau \end{pmatrix}_L & e_R, \mu_R, \tau_R \end{array} \tag{95}$$

  and the repetition of generations.

- The complex pattern of masses and angles suggests they may not be fundamental parameters.
- Hints of a new strong interaction (Technicolor) and the resulting composite scalar particles.

To this we may add the most potent question of all, Why not?

### *21.1 A Prototype Theory of Composite Quarks or Leptons*

Building on our knowledge of gauge theories for the interactions of fundamental fermions, we imagine[81] a set of massless, pointlike, spin-1/2 *preons* carrying the charge of a new gauge interaction called *metacolor*. The metacolor interaction arises from a gauge symmetry generated by the group $\mathcal{G}$. We assume that the metacolor interaction is asymptotically free and infrared confining. Below the characteristic energy scale $\Lambda^*$, the metacolor interaction become strong (in the sense that $\alpha_M(\Lambda^{*2}) \approx 1$) and binds the preons into metacolor-singlet states including the observed quarks and leptons. In this way, the idea of composite quarks and leptons may be seen as a natural extension of the technicolor strategy for composite Higgs scalars.

We expect from the small size of the quarks and leptons that the characteristic energy scale for preon confinement must be quite large,

$$\Lambda^* \gtrsim 1/R \gtrsim 1 \text{ TeV} \ . \tag{96}$$

On this scale, the quarks and leptons are effectively massless. This is the essential fact that a composite theory of quarks and leptons must explain: the quarks and leptons are both small and light.

In general, it is the scale $\Lambda^*$ that determines the masses of composite states. However, there are special circumstances in which some composite states will be exactly or approximately massless compared to the scale $\Lambda^*$. The Goldstone theorem [82] asserts that a massless spin-zero particle arises as a consequence of the spontaneous breakdown of a continuous global symmetry. We have already seen examples of this behavior in the small masses of the color-singlet technipions, which arise as Goldstone bosons when the chiral symmetry of tecchnicolor is spontaneously broken.

't Hooft noted that under certain special conditions, confining theories that possess global chiral symmetries may lead to the existence of massless composite fermions when the chiral symmetries are not spontaneously broken. The key to this observation is the anomaly condition [83] which constrains the pattern of chiral symmetry breaking and the spectrum of light composite fermions:

> For any conserved global (flavor) current, the same anomaly must arise from the fundamental preon fields and from the "massless" physical states.

The existence of an anomaly therefore implies a massless physical state associated with the anomalous charge $Q$. If the (global) chiral or flavor symmetry respected by the preons is broken down when the metacolor interaction becomes strong as

$$G_f \to S_f \subseteq G_f \text{ at } \Lambda^* \ , \tag{97}$$

then the consistency condition can be satisfied in one of two ways:

- If the anomalous charge $Q \notin S_f$, so the global symmetry which has the anomaly is spontaneously broken, then a Goldstone boson arises with specified couplings to the anomaly;
- If instead $Q \in S_f$, so that the anomalous symmetry remains unbroken when metacolor becomes strong, then there must be massless, spin-$\frac{1}{2}$ fermions in the physical spectrum which couple to $Q$ and reproduce the anomaly as given by the preons.

The anomaly conditions thus show how massless fermions might arise as composite states in a strongly interacting gauge theory. In analogy with the case of the pions, we may then suppose that a small bare mass for the preons, or preon electroweak interactions that explicitly break the chiral symmetries, can account for the observed masses of quarks and leptons. However, there is as yet no realistic model of the quark and lepton spectrum. It is natural to ask whether the repeated pattern of generations might be an excitation spectrum. The answer seems clearly to be No. For a strong gauge interaction, all the excitations should occur at a scale $\Lambda^*$ and above.

The scenario that emerges from this rather sketchy discussion of composite models is that all quarks and leptons are massless in some approximation. Generations arise not from excitations, but because of symmetries coupled with the anomaly condition. All masses and mixings arise because of symmetry breaking not associated with the composite strong force. This is a promising outcome on two out of three counts: We may hope for some insight into the near masslessness of quarks and leptons, and into the meaning of generations, but the origin of mass and mixings seems as mysterious as ever.

### *21.2 Manifestations of Compositeness*

The classic test for substructure is to search for form factor effects, or deviations from the expected pointlike behavior in gauge-boson propagators and fermion

vertices.[84] Such deviations would occur in any composite model, at values of $\sqrt{\hat{s}} \gg \Lambda^*$, for example as a consequence of vector meson dominance. In a favored parametrization of this effect, the gauge field propagator is modified by a factor

$$F(Q^2) = 1 + Q^2/\Lambda^{*2} \ , \tag{98}$$

where $Q$ is the four-momentum carried by the gauge field. Measurements of the reactions

$$e^+e^- \to \begin{cases} q\overline{q} \\ \ell^+\ell^- \end{cases} \tag{99}$$

on and off the $Z^0$ yield limits on the compositeness scale which translate into the bound on fermion size given in (94).

Many other tests of compositeness can be carried out in the study at low energies of small effects or rare transitions sensitive to virtual processes. For example, if a composite fermion $f$ is naturally light because of 't Hooft's mechanism, there will arise a contribution to its anomalous magnetic moment of order[85] $(m_f/\Lambda^*)^2$. The close agreement[86] between the QED prediction and the measured value of $(g-2)_\mu$ implies that

$$\Lambda^* \gtrsim 670 \text{ GeV} \tag{100}$$

for the muon. This is the only constraint on $\Lambda^*$ from anomalous moments that improves on the limits from the reactions (99). Within specific models, very impressive bounds on the compositeness scale may be derived from the absence of flavor-changing neutral current transitions.

The observations at PEP, PETRA, and TRISTAN lead to

$$\Lambda^* > 1.7 \text{ to } 4.5 \text{ TeV} \tag{101}$$

for individual channels, and to

$$\Lambda^* > 2.9 \text{ to } 5.4 \text{ TeV} \tag{102}$$

when $e, \mu, \tau$ are combined.[87] LEP measurements also lead to bounds of several TeV.[88] At LEP II, 1 fb$^{-1}$ of running should yield sensitivity up to about 7 TeV.

At energies below those for which form factor effects become characteristic, *i.e.*, for

$$\sqrt{\hat{s}} \sim \text{ few times } \Lambda^*, \tag{103}$$

we may anticipate resonance formation and multiple production. The latter might well include reactions such as

$$u\overline{u} \to \begin{cases} u\overline{u}u\overline{u} \\ u\overline{u}e\overline{e} \\ q^*\overline{q}^* \end{cases} \ , \tag{104}$$

*etc.* In some ways, these would be the most direct and dramatic manifestations of compositeness.

At energies small compared to the compositeness scale, the interaction between bound states is governed by the finite size of the bound states, by the radius $R$. Because the interactions are strong only within this confinement radius, the cross section for scattering composite particles at low energies should be essentially geometric,

$$\sigma \sim 4\pi R^2 \sim 4\pi/\Lambda^{*2} \ . \tag{105}$$

Regarded instead in terms of the underlying field theory, the low energy interaction will be an effective four-fermion interaction, mediated by the exchange of massive bound states of preons. When

$$\sqrt{\hat{s}} \ll \Lambda^*, \tag{106}$$

the resulting interaction will be a contact term, similar to the low-energy limit of the electroweak theory. The general form of the contact interaction will be

$$\mathcal{L}_{\rm contact} \sim \frac{g^2_{\rm Metacolor}}{M_V^2} \cdot \overline{f}_4 \gamma_\mu f_2 \overline{f}_3 \gamma^\mu f_1 \ . \tag{107}$$

Identifying $M_V \approx \Lambda^*$ and

$$g_M^2/4\pi = 1 \ , \tag{108}$$

we see that this interaction reproduces the expected geometrical size of the cross section in the limit (106).

### *21.3 Signals for Compositeness in $p^{\pm}p$ Collisions*

The flavor-diagonal contact interactions symbolized by (107) will modify the cross sections for $ff$ elastic scattering. If in the standard model this process is controlled by a gauge coupling $\alpha_f \ll 1$, then the helicity-preserving pieces of the contact interaction give rise to interference terms in the integrated cross section for $ff$ scattering that are of order [89]

$$\frac{\hat{s}}{\Lambda^{*2}} \cdot \frac{g^2}{4\pi\alpha_f} \equiv \frac{\hat{s}}{\alpha_f \Lambda^{*2}} \tag{109}$$

relative to the standard model contribution. This modification to the conventional expectation is far more dramatic than the anticipated $O(\hat{s}/\Lambda^{*2})$ form factor effects. The direct contact term itself will dominate for (sub)energies satisfying

$$\hat{s} \gtrsim \alpha_f \Lambda^{*2} \ . \tag{110}$$

The approximation that the composite interactions can be represented by contact terms can of course only be reasonable when (106) is satisfied.

Although various flavor-changing contact interactions can be tuned away in particular models (and must be, in many cases, to survive experimental constraints), the flavor-diagonal contact interactions that originate in the exchange of common preons must in general survive. This suggests a strategy for testing the idea of compositeness:

> Consider only four-fermion interactions that are flavor-preserving and respect the $SU(3)_c \otimes SU(2)_L \otimes U(1)_Y$ gauge symmetry of the standard model.

These are unavoidable in a theory capable of producing massless fermionic bound states. Three cases are to be considered:

- electron compositeness;
- quark compositeness;
- common lepton-quark compositeness.

The second and third, which can be attacked effectively in hadron-hadron collisions, will be our concern here.

In the case of quark-quark scattering, we look for deviations from the consequences of QCD for the production of hadron jets. The most general contact interactions that respect the gauge symmetry of the standard model, involve only up and down quarks, and are helicity preserving, involve ten independent terms. Let us consider one of these as an example of the phenomena to be anticipated in a composite world:

$$\mathcal{L}^{(0)}_{\text{contact}} = \eta_0 \cdot \frac{g^2}{2\Lambda^{*2}} \overline{q}_L \gamma^\mu q_L \overline{q}_L \gamma_\mu q_L \ , \tag{111}$$

where $g^2/4\pi \equiv 1$ and $\eta_0 = \pm 1$. This interaction modifies the amplitudes for the transitions

$$\begin{array}{ccccc} & & u\overline{u} \to u\overline{u} & d\overline{d} \to d\overline{d} & \\ uu \to uu & dd \to dd & \overline{uu} \to \overline{uu} & & \overline{dd} \to \overline{dd} \\ & & u\overline{u} \to d\overline{d} & & \\ ud \to ud & u\overline{d} \to u\overline{d} & & \overline{u}d \to \overline{u}d & \\ & & \overline{u}\overline{d} \to \overline{u}\overline{d} & & \end{array} \tag{112}$$

but has no effect on processes involving gluons.

It is convenient to write the differential cross section for the parton-parton scatteing process as

$$\frac{d\hat{\sigma}(ij \to i'j')}{d\hat{t}} = \frac{\pi}{\hat{s}^2} \left| A(ij \to i'j') \right|^2 \ . \tag{113}$$

Then in the presence of a contact term (111) the squares of amplitudes are

$$\begin{aligned} |A(ud \to ud)|^2 &= \left| A(u\overline{d} \to u\overline{d}) \right|^2 \\ &= |A(\overline{u}d \to \overline{u}d)|^2 = \left| A(\overline{u}\overline{d} \to \overline{u}\overline{d}) \right|^2 \\ &= \frac{4}{9}\alpha_s^2(Q^2)\frac{\hat{s}^2+\hat{u}^2}{\hat{t}^2} + \left[\frac{\eta_0 \hat{u}}{\Lambda^{*2}}\right]^2 \ ; \end{aligned} \tag{114}$$

$$\begin{aligned} \left| A(u\overline{u} \to d\overline{d}) \right|^2 &= \left| A(d\overline{d} \to u\overline{u}) \right|^2 \\ &= \frac{4}{9}\alpha_s^2(Q^2)\frac{\hat{t}^2+\hat{u}^2}{\hat{u}^2} + \left[\frac{\eta_0 \hat{u}}{\Lambda^{*2}}\right]^2 \ ; \end{aligned} \tag{115}$$

$$\begin{aligned} |A(u\overline{u} \to u\overline{u})|^2 &= \left| A(d\overline{d} \to d\overline{d}) \right|^2 \\ &= \frac{4}{9}\alpha_s^2(Q^2)\left[\frac{\hat{u}^2+\hat{s}^2}{\hat{t}^2} + \frac{\hat{u}^2+\hat{t}^2}{\hat{s}^2} - \frac{2\hat{u}^2}{3\hat{s}\hat{t}}\right] \\ &\quad + \frac{8}{9}\alpha_s(Q^2)\frac{\eta_0}{\Lambda^{*2}}\left[\frac{\hat{u}^2}{\hat{t}} + \frac{\hat{u}^2}{\hat{s}}\right] + \frac{8}{3}\left[\frac{\eta_0 \hat{u}}{\Lambda^{*2}}\right]^2 \ ; \end{aligned} \tag{116}$$

$$\begin{aligned} |A(uu \to uu)|^2 &= |A(dd \to dd)|^2 \\ &= |A(\overline{u}\overline{u} \to \overline{u}\overline{u})|^2 = \left| A(\overline{d}\overline{d} \to \overline{d}\overline{d}) \right|^2 \qquad (117) \\ &= \frac{4}{9}\alpha_s^2(Q^2)\left[\frac{\hat{u}^2+\hat{s}^2}{\hat{t}^2} + \frac{\hat{s}^2+\hat{t}^2}{\hat{u}^2} - \frac{2\hat{s}^2}{3\hat{u}\hat{t}}\right] \qquad (118) \\ &\quad + \frac{8}{9}\alpha_s(Q^2)\frac{\eta_0}{\Lambda^{*2}}\left[\frac{\hat{s}^2}{\hat{t}} + \frac{\hat{s}^2}{\hat{u}}\right] + \left[\frac{\eta_0}{\Lambda^{*2}}\right]^2\left(\hat{u}^2+\hat{t}^2+\frac{2}{3}\hat{s}^2\right) \ . \end{aligned}$$

Relative to the QCD terms, the influence of the contact term grows linearly with the square $\hat{s}$ of the parton-parton subenergy. Because the contact term modifies the cross section for (anti)quark–(anti)quark scattering, its effects are most apparent at the large values of $p_\perp$ for which valence quark interactions dominate the jet cross section. The search for such enhancements has become a routine part of the comparison between jet cross sections and QCD.[90]

If quarks and leptons have a common preon constituent, the familiar Drell-Yan contribution to dilepton production will be modified by a contact term. Whereas the conventional Drell-Yan contribution falls rapidly with $\mathcal{M}$ (because both parton luminosities and the elementary cross section do), the cross sections including the contact interaction nearly flatten out. The weak dependence upon the effective mass of the lepton pair results from the convolution of the rising elementary cross section with the falling parton luminosities. There are no conventional backgrounds to this signal for quark and lepton substructure.

The contributions of contact terms to dilepton production and jet production are comparable. However, in jet production there are large incoherent QCD contributions from quark-gluon and gluon-gluon interactions. In addition, the standard model cross section for $q\overline{q} \to \ell^+\ell^-$ is smaller than the quark-quark scattering cross section by a factor of order $(\alpha_{EM}/\alpha_s)^2$. This accounts for the greater prominence of the compositeness signal in dilepton production.

**Problem:** How would nearby new strong dynamics affect precision electroweak measurements? To be specific, consider the effect of a contact interaction, as depicted here

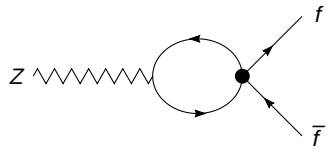


on the decay rate for $Z^0 \to f\bar{f}$. Can the excellent agreement between experiment and the standard-model predictions for $\Gamma(Z^0 \to f\bar{f})$ be used to rule out a low compositeness scale? What deviations from the standard model would you expect if the compositeness scale were no more than a few TeV?

## 22 The Open Questions

I close this brief survey of the physics accessible to hadron colliders with a catalogue of some of the important questions we face. The central challenge in particle physics is to explore the 1-TeV scale, and there to elucidate the nature of electroweak symmetry breaking. Because the agent of electroweak symmetry breaking in the minimal electroweak theory is the Higgs boson, we may abbreviate this problem as the problem of the Higgs sector. We have recognized the significance of the 1-TeV scale—the realm of electroweak symmetry

breaking—for nearly two decades. Through the development of superconducting magnets, and thanks to the experience gained in operating high-energy $\bar{p}p$ colliders at CERN and Fermilab and the evolution of detector architecture from Mark I at SPEAR up through UA1 and UA2 at CERN and CDF and DØ at Fermilab, we now have in hand the technical means to begin our assault on this frontier of our understanding. We have also made great strides in Monte Carlo tools to design and extract physics results from detectors, and in our ability to calculate multiparton amplitudes. But the biggest changes in the way we think about the opportunities of supercollider physics stem from

- the development of silicon microvertex detectors to tag and measure heavy flavors, and
- the great mass of the top quark.

What we seek is an understanding of the distinction between the weak and electromagnetic interactions in the everyday world, an understanding of the origin of masses of the gauge bosons. We can be confident that important clues will be found at the LHC.

It is less certain that the key to the pattern of quarks and lepton masses will be found at a nearby mass scale, but I am encouraged by the great mass of the top quark to believe that we may find a common resolution of the problems of boson and fermion masses. At least I think it is likely that an intensive study of the top quark will provide crucial hints into the puzzle of fermion masses.

Looking beyond the questions we are able to frame with precision, we need to understand the origin and meaning of *CP*-violation, the (possibly related) significance of quark-lepton generations, the origin of the observed gauge symmetries and, specifically, the reason for parity violation in the weak interactions.

By opening up new domains of high energy and short distance, hadron colliders lead us to the realm of pure exploration: to the search for new forces and new forms of matter, and to test of the notion that quarks and leptons might be composite, rather than fundamental.

Let the exploration begin!

## Acknowledgments

I am grateful to R. Michael Barnett and the Particle Data Group for perimission to reproduce Figure 3. I thank Mary Hall Reno for prparing Figures 4 and 5.

Fermilab is operated by Universities Research Association, Inc., under contract DE-AC02-76CHO3000 with the U.S. Department of Energy. I am

grateful to Princeton University for warm hospitality during the writing of these notes. I thank the organizers and students for a stimulating week in Maó.

## References

1. R. Miquel, *These Proceedings.*
2. *Muon Muon Collider: Feasibility Study,* BNL–52503, FERMILAB–CONF–96/092, LBNL–38946 (June 18, 1996). For current information, see http://www.cap.bnl.gov/mumu/mu_home_page.html or http://waldo.fnal.gov/MUMU/mumu.html.
3. An excellent starting place for explorations of the 1-TeV scale is E. Eichten, I. Hinchliffe, K. Lane, and C. Quigg, *Rev. Mod. Phys.* **56**, 579 (1984).
4. For textbook treatments of the electroweak theory, see C. Quigg, *Gauge Theories of the Strong, Weak, and Electromagnetic Interactions* (Addison–Wesley, Reading, Mass., 1983); T.-P. Cheng and L.-F. Li, *Gauge Theory of Elementary Particle Physics* (Oxford University Press, Oxford, 1984); I. J. R. Aitchison and A. J. G. Hey, *Gauge Theories in Particle Physics: A Practical Introduction,* second edition (Adam Hilger, Bristol, 1989).
5. Lower bounds on the Higgs mass date from the work of A. D. Linde, *Zh. Eksp. Teor. Fiz. Pis'ma Red.* **23,** 73 (1976) [*JETP Lett.* **23,** 64 (1976)]; S. Weinberg, *Phys. Rev. Lett.* **36**, 294 (1976). For a review of lower bounds deduced from the requirement of vacuum stability of electroweak potentials, see M. Sher, *Phys. Rep.* **179**, 273 (1989). For useful updates in light of the large mass of the top quark ($m_t \approx 175$ GeV/$c^2$), see G. Altarelli and G. Isidori, *Phys. Lett.* **B337**, 141 (1994); J. Espinosa and M. Quirós, *Phys. Lett.* **B353**, 257 (1995).
6. B. W. Lee, C. Quigg, and H. B. Thacker, *Phys. Rev. D***16**, 1519 (1977). For a somewhat different approach that leads to similar constraints on the mass of the Higgs boson, see M. Veltman, *Acta Phys. Polon. B***8**, 475 (1977).
7. See, for example, M. Chanowitz and M. K. Gaillard, *Nucl. Phys.* **B261**, 279 (1985); M. Chanowitz, M. Golden, and H. Georgi, *Phys. Rev. D***36**, 1490 (1987); *Phys. Rev. Lett.* **57**, 2344 (1986).
8. F. E. Close, *An Introduction to Quarks and Partons* (Academic, New York, 1979); J. L. Rosner, "Quark Models," in *Techniques and Concepts of High Energy Physics,* St. Croix, 1980, edited by T. Ferbel (Plenum, New York, 1981), p. 1.; C. Quigg, "Models for Hadrons," lectures given

at l'Ecole d'Eté de Physique Théorique, Les Houches, in *Gauge Theories in High Energy Physics,* edited by M. K. Gaillard and R. Stora (North-Holland, Amsterdam, 1983), p. 645.

9. Estia J. Eichten, Ian Hinchliffe, and Chris Quigg, *Phys. Rev. D***45**, 2269 (1992). For a recent survey, see T. P. Cheng and Ling-Fong Li, "Chiral quark model of nucleon spin flavor structure with $SU(3)$ and axial $U(1)$ breakings" (electronic archive: hep–ph/9701248).
10. R. M. Barnett, *et al.* (Particle Data Group). *Phys. Rev. D***54**, 1 (1996).
11. H. L. Lai, *et al.* (CTEQ Collaboration), *Phys. Rev. D***55**, 1280 (1997).
12. G. Altarelli and G. Parisi, *Nucl. Phys.* **B126**, 298 (1977).
13. The standard form of the Altarelli-Parisi equations and the Mellin transform method of solution in terms of moments of the parton distributions are treated in C. Quigg, *Gauge Theories of the Strong, Weak, and Electromagnetic Interactions* (Benjamin / Cummings, Reading, Mass., 1983).
14. S. W. Herb, *et al.*, *Phys. Rev. Lett.* **39**, 252 (1977).
15. F. Abe, *et al.* (CDF Collaboration), *Phys. Rev. Lett.* **74**, 2626 (1995).
16. S. Abachi, *et al.* (DØ Collaboration), *Phys. Rev. Lett.* **74**, 2632 (1995).
17. For reviews, see S. J. Wimpenny and B. L. Winer, *Ann. Rev. Nucl. Part. Sci.* **46**, 149 (1996); C. Campagnari and M. Franklin, *Rev. Mod. Phys.* **69**, 137 (1997); B. Carithers and P. Grannis, "Discovery of the Top Quark," Stanford Linear Accelerator *Beam Line* **25,** No. 3, p. 4 (Fall 1995).
18. M. Kobayashi and T. Maskawa, *Prog. Theoret. Phys. (Kyoto)* **49,** 652 (1973).
19. M. Veltman, *Nucl. Phys.* **B123**, 89 (1977); M. S. Chanowitz, M. A. Furman, and I. Hinchliffe, *Nucl. Phys.* **B153**, 402 (1979).
20. See the top-quark full listings in the 1994 and 1996 Reviews of Particle Properties: Particle Data Group, *Phys. Rev. D***50**, 1173 (1994); *ibid.* **54**, 1 (1996). I have combined in quadrature statistical uncertainties and those arising from variations in the Higgs-boson mass. The most recent CDF measurement is reported in J. Lys, Fermilab–Conf–96/409–E; the latest DØ point is from S. Abachi, *et al.* (DØ Collaboration), Fermilab–Pub–97/059–E (electronic archive: hep–ex/9703008).
21. The LEP Collaborations, LEP Electroweak Working Group, and the SLD Heavy Flavor Group, "A Combination of Preliminary Electroweak Measurements and Constraints on the Standard Model," CERN–PPE/96–183 (December 1996). I thank Joachim Mnich for providing the figure.
22. For the underlying calculations, see A. J. Buras and M. Lautenbacher, *Phys. Lett.* **B318**, 212 (1993); A. J. Buras and M. K. Harlander, "A Top Quark Story," in *Heavy Flavours,* edited by A. J. Buras and M. Lindner (World Scientific, Singapore, 1992), p. 58. The band arises from varying

theoretical parameters within the following limits: $B_K = 0.75 \pm 0.15$, $|V_{cb}| = 0.040 \pm 0.003$, $|V_{ub}/V_{cb}| = 0.08 \pm 0.02$, $\Lambda_{\overline{\rm MS}} = 0.2$ – 0.35 GeV, $m_s(m_c) = (160 \pm 20)$ MeV/$c^2$, $B_6 = 1.0 \pm 0.2$, $B_8 = 1.0 \pm 0.2$. I thank Gerhard Buchalla for the computation.

23. G. D. Barr, *et al.* (NA31 Collaboration), *Phys. Lett.* **B317**, 233 (1993); L. K. Gibbons, *et al.* (E731 Collaboration), *Phys. Rev. Lett.* **70**, 1203 (1993).
24. L. Alvarez-Gaumé, J. Polchinski, and M. B. Wise, *Nucl. Phys.* **B221**, 495 (1983), found that electroweak symmetry would be spontaneously broken provided 55 GeV/$c^2 \lesssim m_t \lesssim 200$ GeV/$c^2$.
25. E. Laenen, J. Smith, and W. van Neerven, *Nucl. Phys.* **B369**, 543 (1992), *Phys. Lett.* **B321**, 254 (1994); S. Catani, *et al.*, *Phys. Lett.* **B378**, 329 (1996), *Nucl. Phys.* **B478**, 273 (1996); E. L. Berger and H. Contopanagos, in *QCD and High-Energy Hadronic Interactions,* Proceedings of the XXXI Rencontres de Moriond, edited by J. Trân Thanh Vân (Éditions Frontières, Gif/Yvette, 1996), p. 33 (electronic archive: hep–ph/9605212). For the NLO predictions without resummation, see R. K. Ellis, *Phys. Lett.* **B259**, 492 (1991).
26. S. Parke, "Summary of Top Quark Physics," in *The Albuquerque Meeting: Proceedings of DPF94,* edited by Sally Seidel (World Scientific, Singapore, 1995), p. 726 (electronic archive: hep–ph/9409312).
27. I thank Eric Laenen for providing these calculations.
28. I. Bigi, Yu. L. Dokshitzer, V. Khoze, J. Kühn, and P. Zerwas, *Phys. Lett.* **B181**, 157 (1986). For the QCD corrections, see M. Jeżabek and J. Kühn, *Nucl. Phys.* **B314**, 1 (1989), *Phys. Rev. D***48**, 1910 (1993).
29. Robert A. Nelson, "Guide for Metric Practice," *Phys. Today* **46**, BG15 (August, 1993); Particle Data Group, *Phys. Rev. D***50**, 1173 (1994), p. 1240.
30. V. S. Fadin and V. A. Khoze, *ZhETF Pis'ma* **46**, 417 (1987) [English translation: *JETP Lett.* **46**, 525 (1987)] and *Yad. Fiz.* **48**, 487 (1988) [English translation: *Sov. J. Nucl. Phys.* **48**, 309 (1988)], have noted that the large width of a heavy top quark acts as an infrared cutoff that justifies the application of perturbative QCD. For applications near threshold in $e^+e^- \to t\bar{t}$, see M. J. Strassler and M. E. Peskin, *Phys. Rev. D***43**, 1500 (1991); C. R. Schmidt, *Phys. Rev. D***54**, 3250 (1996).
31. F. Abe, *et al.* (CDF Collaboration), *Phys. Rev. D***50**, 2966 (1994); *Phys. Rev. Lett.* **73**, 225 (1994).
32. S. Abachi, *et al.* (DØ Collaboration), *Phys. Rev. Lett.* **74**, 2422 (1995).
33. See the recent CDF and DØ top masses in Ref. [20].
34. The standard-model prediction for $M_W$ for specified values of $m_t$ and

$M_H$ was calculated using ZFITTER 4.8 (D. Bardin, *et al.*, CERN–TH.6443/92). The other input parameters are $\alpha(M_Z^2) = 1/128.89$, the central value of S. Eideman and F. Jegerlehner, PSI–PR–95–1 and BUDKERINP 95–5 (electronic archive: hep–ph/9502298); and $\alpha_s = 0.123$, from S. Bethke, in *Proceedings of the Workshop on Physics and Experiments with Linear $e^+e^-$ Colliders,* edited by F. A. Harris, S. L. Olsen, and S. Pakvasa ((World Scientific, Singapore, 1993)), p. 687. I thank Tatsu Takeuchi for providing this technology.

35. A four-generation model in which the Fermilab top quark is reinterpreted as $t'$ has been described by H. E. Haber, in *'95 Electroweak Interactions and Unified Theories,* Proceedings of the XXX Rencontres de Moriond, edited by J. Trân Thanh Vân (Éditions Frontières, Gif/Yvette, 1995), p. 249 (electronic archive: hep–ph/9506426). See also M. Carena, H. E. Haber, and C. Wagner, *Nucl. Phys.* **B472**, 55 (1996). For a related perspective, see G. W.-S. Hou, "Prospect for Heavy Quarks lighter than $M_W$ at Tevatron and LEP-2," (electronic archive: hep–ph/9605203)
36. Preliminary result of the CDF Collaboration, presented at the 1997 Rencontres de Moriond by D. Gerdes.
37. T. Stelzer and S. Willenbrock, *Phys. Lett.* **B357**, 125 (1995).
38. K. Fujii, T. Matsui, and Y. Sumino, *Phys. Rev. D***50**, 4341 (1994) study a 150-GeV/$c^2$ top. The case $m_t = 175$ GeV/$c^2$ is treated by Y. Sumino, *Acta Phys. Polon. B***25**, 1837 (1994).
39. For the helicity analysis, see G. L. Kane, G. A. Ladinsky, and C. P. Yuan, *Phys. Rev. D***45**, 124 (1992). Prospects for $e^+e^- \to t\bar{t}$ are presented by A. M. Falk and M. E. Peskin, *Phys. Rev. D***49**, 3320 (1994).
40. C. P. Yuan, *Mod. Phys. Lett.* **A10**, 627 (1995).
41. Standard-model (and beyond) predictions for the $t \to gc, Z^0c$, and $\gamma c$ decay rates are given by G. Eilam, J. L. Hewett, and A. Soni, *Phys. Rev. D***44**, 1473 (1991).
42. For a recent treatment of the effects of anomalous $Zt\bar{c}$ couplings, see T. Han, R. D. Peccei, and X. Zhang, *Nucl. Phys.* **B454**, 527 (1995).
43. G. Mahlon and S. Parke, *Phys. Lett.* **B347**, 394 (1995).
44. For $m_t \lesssim M_W - m_b$, standard top decay ($t \to bW^\star$) is a weak process, which would have been swamped by a (hypothetical) semiweak $t \to bP^+$ process. The existence of such a competing decay would have invalidated lower bounds on $m_t$ derived from fruitless searches in the dilepton channel.
45. Although many searches are insensitive to a $P^+ \to c\bar{b}$ decay, it is plausible that the mass of a charged Higgs boson exceeds 43.5 GeV/$c^2$. See the compilation in L. Montanet, *et al.* (Particle Data Group), *Phys. Rev.*

*D***50**, 1173 (1994) and the listings in the 1996 *Review of Particle Physics,* Ref. [20].

46. Searches for nonstandard top decays have already been carried out. See F. Abe, *et al.* (CDF Collaboration), *Phys. Rev. Lett.* **72**, 1977 (1994); *ibid.* **73**, 2667 (1994).
47. Implications of the dead cone for the average charged multiplicity in events containing heavy quarks are presented in B. A. Schumm, Y. L. Dokshitzer, V. A. Khoze, and D. S. Koetke, *Phys. Rev. Lett.* **69**, 3025 (1992).
48. For measurements of the multiplicity in tagged-$b$ events on the $Z^0$ resonance, see R. Akers, *et al.* (OPAL Collaboration), *Z. Phys. C***61**, 209 (1994); K. Abe, *et al.* (SLD Collaboration), *Phys. Rev. Lett.* **72**, 3145 (1994). Tracks arising from $b$-decay are subtracted.
49. All the important features emerge in an $SU(5)$ unified theory that contains the standard-model gauge group $SU(3)_c \otimes SU(2)_L \otimes U(1)_Y$. The final result is more general.
50. The strategy is explained in H. Georgi, H. R. Quinn, and S. Weinberg, *Phys. Rev. Lett.* **33**, 451 (1974).
51. For a fuller development of the influence of standard-model parameters on the everyday world, see R. N. Cahn, *Rev. Mod. Phys.* **68**, 951 (1996).
52. For a recent treatment and comprehensive bibliography, see B. Schrempp and F. Schrempp, *Phys. Lett.* **B299**, 321 (1993).
53. See, for example, M. Carena, M. Olechowski, S. Pokorski, and C. E. M. Wagner, *Nucl. Phys.* **B419**, 213 (1994), *ibid.* **426**, 269 (1994); C. Kolda, L. Roszkowski, J. D. Wells, and G. L. Kane, *Phys. Rev. D***50**, 3498 (1994); V. Barger, M. S. Berger, and P. Ohmann, "Implications of Supersymmetric Grand Unification," Wisconsin preprint MAD/PH/826 (electronic archive: hep–ph/9404297); J. D. Wells and G. L. Kane, *Phys. Rev. Lett.* **76**, 869 (1996); S. Ambrosanio, *et al.*, *Phys. Rev. Lett.* **76**, 3498 (1996).
54. V. Barger and R. J. N. Phillips, *Phys. Lett.* **B335**, 510 (1994).
55. K. Lane, "Top Quarks and Flavor Physics," Boston University preprint BUHEP–95–2 (electronic archive: hep–ph/9501260). An abbreviated version appears in *Proceedings of the 1994 International Conference on High Energy Physics,* edited by Peter J. Bussey and Ian G. Knowles (Institute of Physics, London, 1995), p. 1223.
56. Extended technicolor is outlined in E. Eichten and K. Lane, *Phys. Lett.* **90B**, 125 (1980). The search for technicolor at the Tevatron collider was described (in the context of a smaller top-quark mass) by E. Eichten, I. Hinchliffe, K. Lane, and C. Quigg, *Phys. Rev. D***34**, 1547 (1986). The

idea of walking technicolor can be traced to the work of B. Holdom, *Phys. Rev. Lett.* **60**, 1223 (1988).
57. The idea of topcolor is explained in W. A. Bardeen, C. T. Hill, and M. Lindner, *Phys. Rev. D***41**, 1647 (1990).
58. E. Eichten and K. Lane, *Phys. Lett.* **B327**, 129 (1994).
59. C. T. Hill and S. J. Parke, *Phys. Rev. D***49**, 4454 (1994). The topcolor model is developed in C. T. Hill, *Phys. Lett.* **B345**, 483 (1995).
60. V. L. Ginzburg and L. D. Landau, *Zh. Eksp. Teor. Fiz.* **20,** 1064 (1950).
61. P. W. Higgs, *Phys. Rev. Lett.* **12**, 132 (1964). The parallel between electroweak symmetry breaking and the Ginzburg-Landau theory is drawn carefully in R. E. Marshak, *Conceptual Foundations of Modern Particle Physics* (World Scientific, Singapore, 1993), §4.4.
62. M. Veltman, *Acta Phys. Polon. B***12**, 437 (1981); C. H. Llewellyn Smith, *Phys. Rep.* **105**, 53 (1984).
63. K. G. Wilson, *Phys. Rev. D***3**, 1818 (1971); *Phys. Rev. B***4,** 3184 (1971); K. G. Wilson and J. Kogut, *Phys. Rep.* **12**, 76 (1974).
64. L. Maiani, G. Parisi, and R. Petronzio, *Nucl. Phys.* **B136**, 115 (1978).
65. For a recent review, see U. M. Heller, *Nucl. Phys. B (Proc. Supp.)* **34** (1994) 101 (electronic archive: hep–lat/9311058).
66. For an approachable introduction, see Joseph D. Lykken, "Introduction to Supersymmetry," Lectures given at the Theoretical Advanced Study Institute in Elementary Particle Physics (TASI 96), FERMILAB-PUB-96-445-T (electronic archive: hep–th/9612114).
67. F. Dyson, *J. Math. Phys.* **8**, 1538 (1967).
68. E. H. Lieb, *Bull. Am. Math. Soc.* **22,** 1 (1990).
69. F. Quevedo, "Lectures on Superstring Phenomenology," given at the Fifth Mexican Workshop of Particles and Fields, Puebla, Mexico, 30 Oct - 3 Nov 1995, CERN-TH-96-65-REV (electronic archive: hep–th/9603074).
70. J. Scherk and J. H. Schwarz, *Nucl. Phys.* **B81**, 118 (1974).
71. L. Arnaudon, *et al.*, *1993 IEEE Particle Accelerator Conference:* Proceedings, p. 44.
72. The case for dynamical symmetry breaking is made eloquently by K. Lane, in Proceedings of the 28th International Conference on High Energy Physics, edited by Z. Ajduk and A. K. Wroblewski (World Scientific, Singapore, 1997), p. 367.
73. "Topcolor" is another approach to dynamical symmetry breaking that is inspired by the BCS theory. The strong coupling of a heavy top quark to the Higgs boson raises the possibility that the breaking of electroweak symmetry may be intimately linked with the top quark. For explicit implementations of this idea, see W. A. Bardeen, C. T. Hill, and M. Lind-

ner, *Phys. Rev. D***41**, 1647 (1990); Y. Nambu, in *New Trends in Strong Coupling Gauge Theories,* edited by M. Bando, T. Muta, K. Yamawaki (World Scientific, Singapore, 1989), p 3; Y. Nambu, in *New theories in physics,* edited by Z. Ajduk, S. Pokorski, A. Trautman (World Scientific, Singapore, 1989), p. 1; V. A. Miransky, M. Tanabashi, and K. Yamawaki, *Mod. Phys. Lett. A***4,** 1043 (1989); *Phys. Lett.* **B221**, 177 (1989). C. T. Hill and S. J. Parke, *Phys. Rev. D***49**, 4454 (1994), have emphasized that $t\bar{t}$ interactions may be acutely sensitive to new physics associated with the dynamics of electroweak symmetry breaking.

74. J. Bardeen, L. N. Cooper, and J. R. Schrieffer, *Phys. Rev.* **106,** 162 (1962).
75. Y. Nambu, *Phys. Rev. Lett.* **4**, 380 (1960).
76. M. Weinstein, *Phys. Rev. D***8**, 2511 (1973).
77. S. Weinberg, *Phys. Rev. D***13**, 974 (1976), *ibid.* **19**, 1277 (1979).
78. L. Susskind, *Phys. Rev. D***20**, 2619 (1979).
79. The idea of high-scale, or "walking," extended technicolor developed from the ideas in B. Holdom, *Phys. Rev. D***24**, 1441 (1981), *Phys. Lett.* **150B**, 301 (1985); T. Appelquist, D. Karabali, and L. C. R. Wijewardhana, *Phys. Rev. Lett.* **57**, 957 (1986); T. Appelquist and L. C. R. Wijewardhana, *Phys. Rev. D***36**, 568 (1987); K. Tamawaki, M. Bando, and K. Matumoto, *Phys. Rev. Lett.* **56**, 1335 (1986); T. Akiba and T. Yanagida, *Phys. Lett.* **169B**, 69 (1980). The current state of the technicolor art is summarized in K. Lane, "An Introduction to Technicolor," in *The Building Blocks of Creation: From Microfermis to Megaparsecs,* Proceedings of TASI93, edited by S. Raby and T. P. Walker (World Scientific, Singapore, 1994), p. 381. (electronic archive: hep–ph/9401324). Prospects for uncovering evidence of multiscale technicolor in top production have been discussed recently by E. Eichten and K. Lane, *Phys. Lett.* **B327**, 129 (1994).
80. E. Eichten, K. Lane, and J. Womersley, "Finding Low-Scale Technicolor at Hadron Colliders," FERMILAB-PUB-97/116-T (electronic archive: hep–ph/9704445).
81. The basic ideas of a composite model are explained thoroughly in E. Eichten, R. Peccei, J. Preskill, and D. Zeppenfeld, *Nucl. Phys.* **B268**, 161 (1986). See also G. 't Hooft, in *Recent Developments in Gauge Theories,* edited by G. 't Hooft, *et al.* (Plenum, New York, 1980), p. 135. For a review, see H. Harari, "Composite Quarks and Leptons," in *Fundamental Forces,* Proceedings of the Twenty-Seventh Scottish Universities Summer School in Physics, St. Andrews, 1984, edited by D. Frame and K. Peach (SUSSP Publications, Edinburgh, 1985), p. 357.

82. J. Goldstone, *Nuovo Cim.* **19,** 154 (1960).
83. See S. Coleman and B. Grossman, *Nucl. Phys.* **B203**, 205 (1982) for an investigation of the anomaly condition.
84. M. Chanowitz and S. D. Drell, *Phys. Rev. Lett.* **30**, 807 (1973).
85. R. Barbieri, L. Maiani, and R. Petronzio, *Phys. Lett.* **96B**, 63 (1980); S. J. Brodsky and S. D. Drell, *Phys. Rev. D***22**, 2236 (1980).
86. J. Calmet, *et al.*, *Rev. Mod. Phys.* **49**, 21 (1977); F. Combley, F. J. M. Farley, and E. Picasso, *Phys. Rep.* **68**, 93 (1981).
87. H. Kroha, *Phys. Rev. D***46**, 58 (1992).
88. See the minireview on searches for quark and lepton compositeness on p. 699 of the 1996 *Review of Particle Physics,* Ref. [20].
89. E. Eichten, K. Lane, and M. Peskin, *Phys. Rev. Lett.* **50**, 811 (1983). See also I. Bars and I. Hinchliffe, *Phys. Rev. D***23**, 704 (1986).
90. See F. Abe, *et al.* (CDF Collaboration), *Phys. Rev. Lett.* **77**, 438 (1996), in which a hint of an excess over QCD was reported, and G. C. Blazey (for the DØ Collaboration), FERMILAB-CONF-96/132-E, where cross sections consistent with QCD are reported.